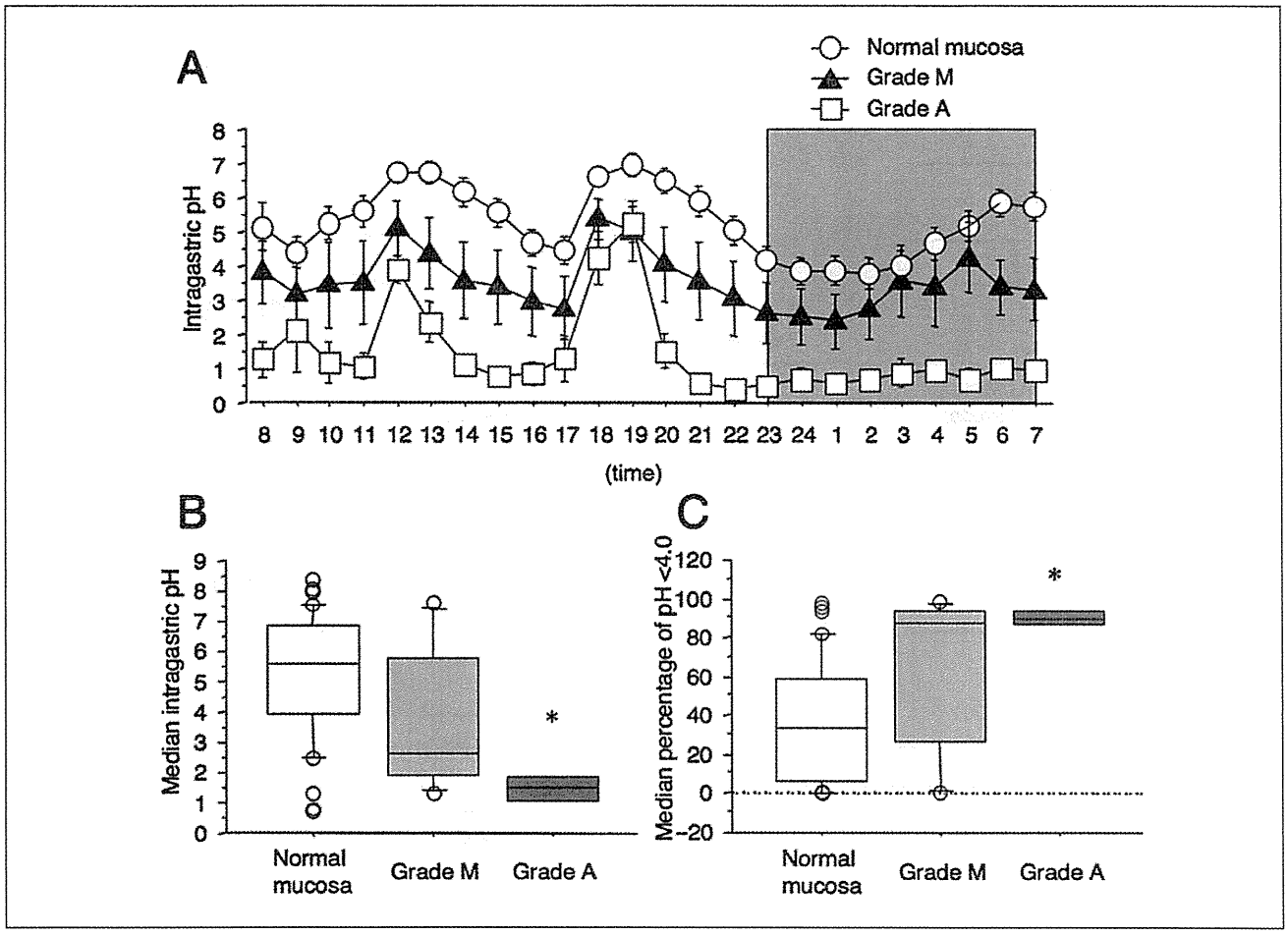

*Figure 3. The median 24-hour pH-time profiles (A), the median intragastric pHs (B), and the median percentage of intragastric pH less than 4.0 (C) in the groups with different endoscopic findings: normal, grade M, and grade A. The median intragastric pH in patients with GERD grade A was significantly lower than that with normal mucosa as determined endoscopically. Similarly, the median percentage of intragastric pH less than 4.0 in patients with GERD grade A was significantly longer than that in patients with normal mucosa as determined endoscopically. *P < .05 (vs normal mucosa group).*

However, it has not been fully elucidated whether low-dose aspirin affects gastric acid secretion[35] and causes GERD or NERD[8,36] and whether a PPI prevents aspirin-induced esophageal mucosal injury as in the cases of other acid-related diseases and NSAID-induced peptic ulcer. In the analysis of a database of more than 100 000 US military veterans with variety of diseases, NSAIDs were found to be significantly associated with the occurrence of esophageal erosions and stricture (eg, osteoarthritis [odds ratio, 1.42; 95% confidence interval, 1.36-1.48]).[8] Avidan et al[36,37] reported that NSAIDs increased the risk for esophageal ulcer and that 21% of eligible patients treated with NSAIDs had GERD. However, epidemiological studies of aspirin users are limited.[38,39] In a Western population, Ruszniewski et al[38] reported that the prevalence of GERD in French adults with aspirin intake was 25%, which was significantly higher than that in nonusers (18%). Unfortunately, there are no data on GERD development by aspirin intake in Asian populations with relatively low acid secretion. As observed in this study, most cases of aspirin-induced GERD involved mild damage, including grade M with endoscopically revealed redness, white granules, and/or edema in the EC junction.[40] Therefore, the endoscopic examination of NERD patients will be required for epidemiological studies of aspirin users in further study.

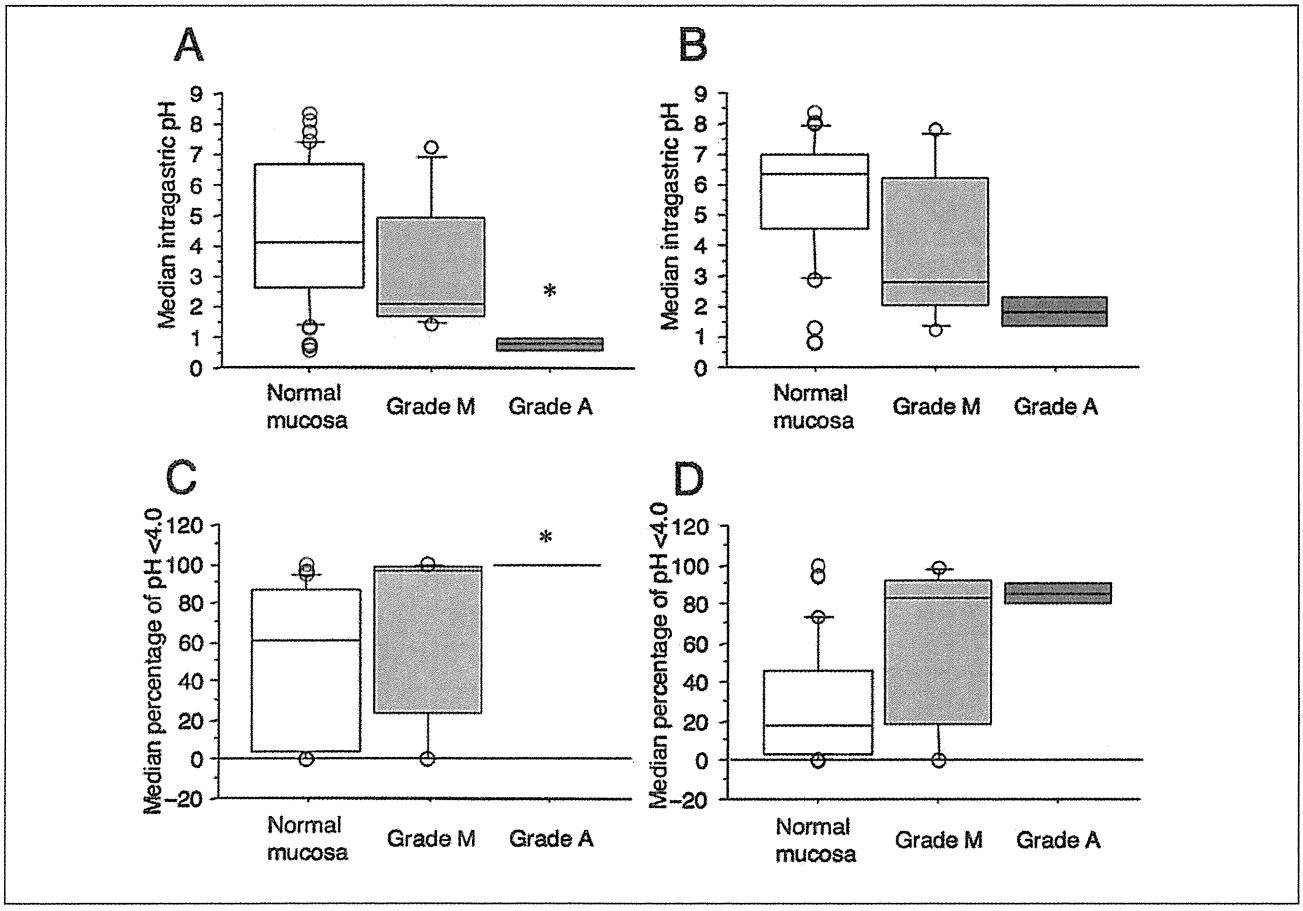

Figure 4. The median intragastric pHs in 3 different GERD groups in nighttime (A) and daytime (B) and the median percentage of intragastric pH less than 4.0 of 3 different GERD groups in nighttime (C) and daytime (D). The concomitant of RPZ once daily dosing with and without aspirin regimens in daytime significantly increased compared with nighttime. Nocturnal gastric pH value was associated with grade of esophageal mucosal injury as determined endoscopically. *P < .05 *(vs normal patients group).*

There are 3 kinds of esophageal defense system: pre-epithelial defense (eg, mucus layer, unstirred water layer, surface bicarbonate ion concentration), epithelial defense (eg, cell membrane, intercellular junction, ion transport, cell proliferation, buffer) and postepithelial defense (eg, blood flow and tissue acid-base status).[41] However, the direct mechanism whereby aspirin causes esophageal mucosal injury is unclear. Semble et al[42] speculated that NSAIDs and aspirin induced esophageal mucosal injury by a direct cellular toxicity that disrupts the mucosal barrier of the esophagus rather than by inhibition of prostaglandins synthesis. However, except in specific conditions, such as diverticulum, achalasia, scleroderma, and humpback, aspirin capsules or tablets will pass the esophagus within 1 to 2 seconds. In this study, although no patients had a passage disorder, around a half of subjects revealed GERD after aspirin intake for 7 days. Gastric prostaglandins (PG) are known to have important roles in protecting gastric mucosa from damage by gastric acid; in esophageal mucosa, the levels of PGE2, one of the main PGs, were reported to significantly decrease by dosing of aspirin.[43,44] Therefore, we speculate that aspirin makes the esophageal mucosa vulnerable by decreasing esophageal prostaglandin levels and that the exposure of refluxed gastric contents to esophageal mucosa will easily break the esophageal mucosal barrier, as observed in gastric mucosa. To clarify this mechanism, further study is required.

PPIs are absorbed in the small intestine and via the systemic circulation reach the gastric parietal cells, where they bind irreversibly to H^+/K^+-ATPase and disturb its function, thereby resulting in a potent

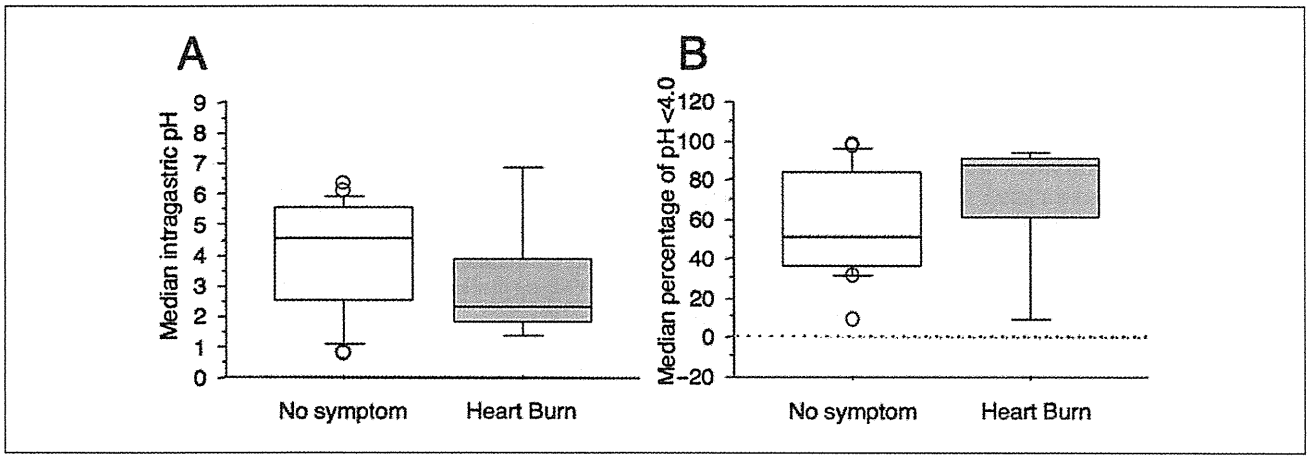

Figure 5. The median intragastric pHs (A) and the median percentage time for intragastric pH less than 4.0 (B) in subjects with and without GERD symptoms.

Table IV Pathological Finding of Esophageal Mucosa by Different Treatment Regimens

Treatment Regimen	Inflammatory Cell Infiltration	Dilatation of Vascular Vessel
Placebo	0 (0-1), 13.3	0 (0-2), 6.7
RPZ 10 mg	0 (0-1), 26.7	0 (0-1), 26.7
Aspirin	0 (0-2), 46.7	0 (0-2), 46.7
Aspirin + RPZ 10 mg once daily	0 (0-1), 33.3	0 (0-2), 20.0
Aspirin + RPZ 10 mg 4 times daily	0 (0-1), 26.7	0 (0-2), 26.7

RPZ, rabeprazole. Data given as median (range), percentage of positive patients. There were no significant differences in inflammatory cell infiltration or dilatation of vascular vessel among the different treatment regimens.

Table V Pathological Findings Among Different Severities of Gastroesophageal Reflux Disease (GERD) and Nonerosive GERD (NERD)

	Inflammatory Cell Infiltration	Dilatation of Vascular Vessel
Normal endoscopic findings	0 (0-2), 26.2	0 (0-2), 19.7
NERD grade N[a]	0 (0-1), 33.3	0 (0-2), 33.3
NERD grade M	0 (0-1), 33.3	1 (0-2), 55.6
GERD grade A	1 (1-1), 100	0.5 (0-1), 50.0

Data given as median (range), percentage of positive patients. There were no significant differences among treatment regimens.
a. NERD grade N was patients with gastroduodenal symptom who revealed no mucosal change in endothelial cell junction.

acid inhibition throughout a 24-hour period. PPIs undergo extensive hepatic metabolism mainly by CYP2C19 and, therefore, the polymorphism of CYP2C19 influenced pharmacokinetics and pharmacodynamics of PPIs. Moreover, rates of *H pylori* eradication and GERD cure are known to differ among different CYP2C19 genotype.[24] Although intragastric pH should be maintained at greater than 4.0 by acid-inhibitory drugs to prevent esophageal mucosal damage,[20] in this study when we used the concomitant regimen of RPZ and aspirin, RPZ 10 mg once daily effectively prevented the aspirin-induced esophageal mucosal injury irrespective of CYP2C19 genotype status. We believe that this occurred because rabeprazole was mainly metabolized by a nonenzymatic pathway and RPZ 10 mg once daily dosing could inhibit gastric acid secretion not only for CYP2C19 IM and PM but also for RM. Importantly, aspirin-induced GERD/NERD were cured by potent acid inhibition, the same as acid-related disease. Therefore, we assume that RPZ 10 mg once daily dosing may prevent esophageal mucosal injury by low-dose aspirin in Japanese subjects. Moreover, when lansoprazole and omeprazole are selected with aspirin, it is advisable to consider CYP2C19 genotype status.

Patients with acute myocardial infarction receiving low-dose aspirin are often concomitantly dosed with a calcium antagonist (80.8%) and nitrates (84.0%).[45] Both drugs often induce GERD by relaxing the lower esophageal sphincter and/or impairing esophageal clearance of regurgitated gastric contents.[46] Moreover, the defense system of esophageal mucosa in many older people is insufficient. In this

study, surprisingly, about half of healthy young subjects developed GERD after only 7 days of low-dose aspirin. Although we had no data for an older population, the risk of aspirin-induced mucosal injury in older patients is assumed to be much higher than that in younger subjects. Therefore, potent acid inhibition by a PPI and careful observation are required for older patients treated with low-dose aspirin.

Around a half of aspirin users receive other anticoagulant drugs, such as warfarin potassium clopidogrel, for arteriosclerosis, angina pectoris, and brain infarction. Concomitant use of aspirin with other anticoagulant drugs increases the risk of gastrointestinal bleeding compared with aspirin alone. Therefore, patients often experience massive hemorrhage from either peptic ulcers or gastric erosions. We suggest that to prevent such gastrointestinal events, concomitant treatment with a PPI (eg, RPZ 10 mg as suggested by this study) be used. Moreover, aspirin users should undergo endoscopy to prevent potentially destructive gastrointestinal events.

We demonstrated that aspirin induced microscopic changes in inflammatory cell infiltration or dilatation of vascular vessel in esophageal mucosa in about half of subjects dosed with aspirin (59.5% and 53.0%, respectively), even though esophageal mucosa appeared endoscopically normal (normal and grade N). This suggests that patients taking aspirin are at greater risk of esophageal erosion and ulcer compared with patients who do not take aspirin. The concomitant dosage of PPIs microscopically and endoscopically decreased the incidence of esophageal mucosal injury in this study. Our result suggests that half of patients taking aspirin might be dosed with a PPI to prevent aspirin-induced GERD.

In conclusion, we demonstrated that low-dose aspirin could be a risk factor for GERD and that the occurrence of esophageal mucosal injury by low-dose aspirin was closely related to intragastric pH value, especially at night. The disadvantage of this study was the absence of an older population and an *H pylori*–positive population, both of whom are at higher risk for NSAID-associated gastrointestinal complications,[39,47,48] and the absence of intra-esophageal pH values. Whether concomitant therapy with PPI could cost-effectively offset risks for patients and whether concomitant therapy should be selected for all patients taking NSAIDs or aspirin are not known. However, concomitant therapy with PPI might be appropriate for patients treated with low-dose aspirin, especially those at high risk for GERD, such as older patients, patients with hiatus hernia, patients with short-segment Barrett's esophagus, those who take many kinds of NSAIDs, and those who take calcium antagonist and nitrates.

This study was supported by a scientific research grant from the Yokoyama Foundation for Clinical Pharmacology; a grant-in-aid from the Center of Excellence from the Ministry of Education, Culture, Sports, Science and Technology; and a grant-in-aid from the Ministry of Education, Culture, Sports, Science and Technology of Japan (17590470). None of the authors has conflicts of interest related to this study.

Financial disclosure: None declared.

REFERENCES

1. Nasseri-Moghaddam S, Mofid A, Ghotbi MH, et al. Epidemiological study of gastro-oesophageal reflux disease: reflux in spouse as a risk factor. *Aliment Pharmacol Ther.* 2008;28:144-153.

2. Boeckxstaens GE. The pathophysiology of gastro-oesophageal reflux disease. *Aliment Pharmacol Ther.* 2007;26:149-160.

3. Fass R. Erosive esophagitis and nonerosive reflux disease (NERD): comparison of epidemiologic, physiologic, and therapeutic characteristics. *J Clin Gastroenterol.* 2007;41:131-137.

4. Nagahara A, Miwa H, Minoo T, et al. Increased esophageal sensitivity to acid and saline in patients with nonerosive gastroesophageal reflux disease. *J Clin Gastroenterol.* 2006;40:891-895.

5. Miwa H, Sasaki M, Furuta T, et al. Efficacy of rabeprazole on heartburn symptom resolution in patients with non-erosive and erosive gastro-oesophageal reflux disease: a multicenter study from Japan. *Aliment Pharmacol Ther.* 2007;26:69-77.

6. Joh T, Miwa H, Higuchi K, et al. Validity of endoscopic classification of nonerosive reflux disease. *J Gastroenterol.* 2007;42:444-449.

7. Wilkins WE, Ridley MG, Pozniak AL. Benign stricture of the oesophagus: role of non-steroidal anti-inflammatory drugs. *Gut.* 1984;25:478-480.

8. El-Serag HB, Sonnenberg A. Association of esophagitis and esophageal strictures with diseases treated with nonsteroidal anti-inflammatory drugs. *Am J Gastroenterol.* 1997;92:52-56.

9. Ryan P, Hetzel DJ, Shearman DJ, et al. Risk factors for ulcerative reflux oesophagitis: a case-control study. *J Gastroenterol Hepatol.* 1995;10:306-312.

10. Lanas A, Hirschowitz BI. Significant role of aspirin use in patients with esophagitis. *J Clin Gastroenterol.* 1991;13:622-627.

11. Diaz-Rubio M, Moreno-Elola-Olaso C, Rey E, et al. Symptoms of gastro-oesophageal reflux: prevalence, severity, duration and associated factors in a Spanish population. *Aliment Pharmacol Ther.* 2004;19:95-105.

12. Kotzan J, Wade W, Yu HH. Assessing NSAID prescription use as a predisposing factor for gastroesophageal reflux disease in a Medicaid population. *Pharm Res* .2001;18:1367-1372.

13. Hernandez-Diaz S, Rodriguez LA. Association between nonsteroidal anti-inflammatory drugs and upper gastrointestinal tract bleeding/perforation: an overview of epidemiologic studies published in the 1990s. *Arch Intern Med.* 2000;160:2093-2099.

14. Derry S, Loke YK. Risk of gastrointestinal haemorrhage with long term use of aspirin: meta-analysis. *BMJ.* 2000;321:1183-1187.

15. Weil J, Colin-Jones D, Langman M, et al. Prophylactic aspirin and risk of peptic ulcer bleeding. *BMJ.* 1995;310:827-830.

16. Lanza FL, Royer GL Jr, Nelson RS. Endoscopic evaluation of the effects of aspirin, buffered aspirin, and enteric-coated aspirin on gastric and duodenal mucosa. *N Engl J Med.* 1980;303:136-138.

17. Kelly JP, Kaufman DW, Jurgelon JM, et al. Risk of aspirin-associated major upper-gastrointestinal bleeding with enteric-coated or buffered product. *Lancet.* 1996;348:1413-1416.

18. Sorensen HT, Mellemkjaer L, Blot WJ, et al. Risk of upper gastrointestinal bleeding associated with use of low-dose aspirin. *Am J Gastroenterol.* 2000;95:2218-2224.

19. Klinkenberg-Knol EC, Festen HP, Jansen JB, et al. Long-term treatment with omeprazole for refractory reflux esophagitis: efficacy and safety. *Ann Intern Med.* 1994;121:161-167.

20. Bell NJ, Burget D, Howden CW, et al. Appropriate acid suppression for the management of gastro-oesophageal reflux disease. *Digestion.* 1992;51(suppl 1):59-67.

21. Shirai N, Furuta T, Moriyama Y, et al. Effects of CYP2C19 genotypic differences in the metabolism of omeprazole and rabeprazole on intragastric pH. *Aliment Pharmacol Ther.* 2001;15:1929-1937.

22. Furuta T, Ohashi K, Kosuge K, et al. CYP2C19 genotype status and effect of omeprazole on intragastric pH in humans. *Clin Pharmacol Ther.* 1999;65:552-561.

23. Sugimoto M, Furuta T, Shirai N, et al. Different dosage regimens of rabeprazole for nocturnal gastric acid inhibition in relation to cytochrome P450 2C19 genotype status. *Clin Pharmacol Ther.* 2004;76:290-301.

24. Furuta T, Shirai N, Watanabe F, et al. Effect of cytochrome P4502C19 genotypic differences on cure rates for gastroesophageal reflux disease by lansoprazole. *Clin Pharmacol Ther.* 2002;72:453-460.

25. Ishizaki T, Horai Y. Review article: cytochrome P450 and the metabolism of proton pump inhibitors—emphasis on rabeprazole. *Aliment Pharmacol Ther.* 1999;13(suppl 3):27-36.

26. Yasuda S, Horai Y, Tomono Y, et al. Comparison of the kinetic disposition and metabolism of E3810, a new proton pump inhibitor, and omeprazole in relation to S-mephenytoin 4'-hydroxylation status. *Clin Pharmacol Ther.* 1995;58:143-154.

27. Adachi K, Katsube T, Kawamura A, et al. CYP2C19 genotype status and intragastric pH during dosing with lansoprazole or rabeprazole. *Aliment Pharmacol Ther.* 2000;14:1259-1266.

28. Miki K, Ichinose M, Ishikawa KB, et al. Clinical application of serum pepsinogen I and II levels for mass screening to detect gastric cancer. *Jpn J Cancer Res* .1993;84:1086-1090.

29. Sugimoto M, Furuta T, Shirai N, et al. Initial 48-hour acid inhibition by intravenous infusion of omeprazole, famotidine, or both in relation to cytochrome P450 2C19 genotype status. *Clin Pharmacol Ther.* 2006;80:539-548.

30. Sugimoto M, Furuta T, Shirai N, et al. Comparison of an increased dosage regimen of rabeprazole versus a concomitant dosage regimen of famotidine with rabeprazole for nocturnal gastric acid inhibition in relation to cytochrome P450 2C19 genotypes. *Clin Pharmacol Ther.* 2005;77:302-311.

31. Armstrong D, Bennett JR, Blum AL, et al. The endoscopic assessment of esophagitis: a progress report on observer agreement. *Gastroenterology.* 1996;111:85-92.

32. Dixon MF, Genta RM, Yardley JH, et al. Classification and grading of gastritis. The updated Sydney System. International Workshop on the Histopathology of Gastritis, Houston 1994. *Am J Surg Pathol.* 1996;20:1161-1181.

33. de Morais SM, Goldstein JA, Xie HG, et al. Genetic analysis of the S-mephenytoin polymorphism in a Chinese population. *Clin Pharmacol Ther.* 1995;58:404-411.

34. de Morais SM, Wilkinson GR, Blaisdell J, et al. Identification of a new genetic defect responsible for the polymorphism of (S)-mephenytoin metabolism in Japanese. *Mol Pharmacol.* 1994;46:594-598.

35. Savarino V, Mela GS, Zentilin P, et al. Effect of one-month treatment with nonsteroidal antiinflammatory drugs (NSAIDs) on gastric pH of rheumatoid arthritis patients. *Dig Dis Sci.* 1998;43:459-463.

36. Avidan B, Sonnenberg A, Schnell TG, et al. Risk factors for erosive reflux esophagitis: a case-control study. *Am J Gastroenterol.* 2001;96:41-46.

37. Avidan B, Sonnenberg A, Schnell TG, et al. Risk factors of oesophagitis in arthritic patients. *Eur J Gastroenterol Hepatol.* 2001;13:1095-1099.

38. Ruszniewski P, Soufflet C, Barthelerny P, et al. NSAIDs intake is a risk factor for gastroesophageal reflux *Gastroenterology.* 2007;132(suppl 2):M1917.

39. Laine L, Bombardier C, Hawkey CJ, et al. Stratifying the risk of NSAID-related upper gastrointestinal clinical events: results of a double-blind outcomes study in patients with rheumatoid arthritis. *Gastroenterology.* 2002;123:1006-1012.

40. Laine L, Maller E, Yu C, et al. Ulcer formation with low-dose enteric-coated aspirin and the effect of COX-2 selective inhibition: a double-blind trial. *Gastroenterology.* 2004;127:395-402.

41. Orland R. Oesophageal mucosal resistance. *Aliment Pharmacol Ther.* 1998;12:191-197.

42. Semble EL, Wu WC, Castell DO. Nonsteroidal antiinflammatory drugs and esophageal injury. *Semin Arthritis Rheum.* 1989;19:99-109.

43. Poplawski C, Sosnowski D, Szaflarska-Poplawska A, et al. Role of bile acids, prostaglandins and COX inhibitors in chronic esophagitis in a mouse model. *World J Gastroenterol.* 2006;12:1739-1742.

44. Triadafilopouloa G, Kaur B, Sood S, et al. The effects of esomeprazole combined with aspirin or rofecoxib on prostaglandin E2 production in patients with Barrett's oesophagus. *Aliment Pharmacol Ther.* 2006;23:997-1005.

45. Yasue H, Ogawa H, Tanaka H, et al. Effects of aspirin and trapidil on cardiovascular events after acute myocardial infarction. Japanese Antiplatelets Myocardial Infarction Study (JAMIS) Investigators. *Am J Cardiol.* 1999;83:1308-1313.

46. Hongo M, Traube M, McAllister RG Jr, et al. Effects of nifedipine on esophageal motor function in humans: correlation with plasma nifedipine concentration. *Gastroenterology.* 1984;86:8-12.

47. Chan FK, Ching JY, Hung LC, et al. Clopidogrel versus aspirin and esomeprazole to prevent recurrent ulcer bleeding. *N Engl J Med.* 2005;352:238-244.

48. Chan FK, Graham DY. Review article: prevention of non-steroidal anti-inflammatory drug gastrointestinal complications—review and recommendations based on risk assessment. *Aliment Pharmacol Ther* 2004;19:1051-1061.

Lung Cancer 71 (2011) 19–27

Contents lists available at ScienceDirect

Lung Cancer

journal homepage: www.elsevier.com/locate/lungcan

Suppression of hydroxyurea-induced centrosome amplification by NORE1A and down-regulation of NORE1A mRNA expression in non-small cell lung carcinoma

Kazuya Shinmura[a], Hong Tao[a], Kiyoko Nagura[a], Masanori Goto[a], Shun Matsuura[a], Takahiro Mochizuki[b], Kazuya Suzuki[b], Masayuki Tanahashi[c], Hiroshi Niwa[c], Hiroshi Ogawa[d], Haruhiko Sugimura[a,*]

[a] 1st Department of Pathology, Hamamatsu University School of Medicine, 1-20-1 Handayama, Higashi Ward, Hamamatsu 431-3192, Shizuoka, Japan
[b] 1st Department of Surgery, Hamamatsu University School of Medicine, 1-20-1 Handayama, Higashi Ward, Hamamatsu 431-3192, Japan
[c] Division of Thoracic Surgery, Respiratory Disease Center, Seirei Mikatahara General Hospital, 3453 Mikatahara, Kita Ward, Hamamatsu 433-8558, Japan
[d] Division of Pathology, Seirei Mikatahara General Hospital, 3453 Mikatahara, Kita Ward, Hamamatsu 433-8558, Japan

ARTICLE INFO

Article history:
Received 25 January 2010
Received in revised form 1 April 2010
Accepted 2 April 2010

Keywords:
Centrosome amplification
Chromosome instability
Hydroxyurea
mRNA down-regulation
Non-small cell lung carcinoma
NORE1A

ABSTRACT

The candidate tumor suppressor NORE1A is a nucleocytoplasmic shuttling protein, and although a fraction of the NORE1A in cells is localized to their centrosomes, the role of centrosomal NORE1A has not been elucidated. In this study we investigated the role of NORE1A in the numerical integrity of centrosomes and chromosome stability in lung cancer cells. Exposure of *p53*-deficient H1299 lung cancer cell line to hydroxyurea (HU) resulted in abnormal centrosome amplification (to 3 or more centrosomes per cell) as determined by immunofluorescence analysis with anti-γ-tubulin antibody, and forced expression of wild-type NORE1A partially suppressed the centrosome amplification. The nuclear export signal (NES) mutant (L377A/L384A) of NORE1A did not localize to centrosomes and did not suppress the centrosome amplification induced by HU. Fluorescence *in situ* hybridization analyses with probes specific for chromosomes 2 and 16 showed that wild-type NORE1A, but not NES-mutant NORE1A, suppressed chromosome instability in HU-exposed H1299 cells that was likely to have resulted from centrosome amplification. We next examined the status of NORE1A mRNA expression in non-small cell lung carcinoma (NSCLC) and detected down-regulation of NORE1A mRNA expression in 25 (49%) of 51 primary NSCLCs by quantitative real-time-polymerase chain reaction analysis. These results suggest that NORE1A has activity that suppresses the centrosome amplification induced by HU and that NORE1A mRNA down-regulation is one of the common gene abnormalities in NSCLCs, both of which imply a key preventive role of NORE1A against the carcinogenesis of NSCLC.

1. Introduction

NORE1 (*RASSF5*) is a member of the RASSF gene family, and *NORE1A* is the longest and major splice isoform of the *NORE1* gene [1–3]. Its product, NORE1A, is a nucleocytoplasmic shuttling protein and has a growth-suppressive function [4–9]. Interestingly, a fraction of NORE1A is localized to centrosomes [6], but the role of centrosomal NORE1A has never been elucidated. Centrosomes are major microtubule-organizing centers, and at any given time during the cell cycle each cell contains one or two centrosomes [10–13]. When centrosome amplification (to 3 or more centrosomes per cell) occurs as a result of some mechanism, the amplification leads to aberrant mitotic spindle formation, merotelic kinetochore-microtubule attachment errors, lagging chromosome formation, and chromosome missegregation, all of which are thought to be possible causes of chromosome instability (CIN) [12–15]. One of the mechanisms underlying the induction of centrosome amplification is suggested by the fact that centrosomes in cells whose cell cycle has been arrested by exposure to a DNA synthesis inhibitor, *i.e.*, aphidicolin or hydroxyurea (HU), an S-phase entry inhibitor, *i.e.*, mimosine, or DNA damage have been shown to continue to duplicate, resulting in the generation of amplified centrosomes [13,16–20]. Efficient centrosome amplification in arrested cells has also been shown to occur when *p53* is either lost or mutationally inactivated [13,17].

Hypermethylation of the *NORE1A* promoter region has been detected in some types of cancers [2–5,21–23]. Hesson et al. and Irimia et al. found that the *NORE1A* promoter is hypermethylated in 24% and 28%, respectively, of primary non-small cell lung carcinomas (NSCLCs) in studies in which they used the methylation-specific-polymerase chain reaction (MS-PCR) method [22,23]. To our knowledge, however, there have been no report of studies that compared the level of NORE1A mRNA expression in the cancerous tissue of primary NSCLCs and corresponding

* Corresponding author. Tel.: +81 53 435 2220; fax: +81 53 435 2225.
E-mail address: hsugimur@hama-med.ac.jp (H. Sugimura).

0169-5002/$ – see front matter © 2010 Elsevier Ireland Ltd. All rights reserved.
doi:10.1016/j.lungcan.2010.04.006

non-cancerous tissue. Although promoter hypermethylation is a well-known mechanism underlying reductions of gene expression, other factors are also involved in the regulation of the expression level [24–26]. Accordingly, in the present study we investigated the level of NORE1A mRNA expression in primary NSCLCs and in NSCLC cell lines. In addition, since CIN is often observed in NSCLC [27], we hypothesized that centrosomal NORE1A has activity that controls the numerical integrity of centrosomes in NSCLC cells, and we tested this hypothesis in a *p53*-deficient H1299 NSCLC cell line.

2. Materials and methods

2.1. Cell lines, primary cancers, and reagents

An immortalized human airway epithelial cell line, 16HBE14o- (simian virus 40-transformed human bronchial epithelial cells) [28], 8 human adenocarcinoma of the lung cell lines, *i.e.*, cell lines A549, H358, H820, H2087, LC-2/ad, RERF-LC-MS, VMRC-LCD, and RERF-LC-KJ, 3 large cell carcinoma of the lung cell lines, *i.e.*, cell lines H460, H1299, and Lu65, and a squamous cell carcinoma of the lung cell line, cell line ABC-1, were used in this study. Cell line 16HBE14o- was a gift from Dr. D.C. Gruenert (California Pacific Medical Center Research Institute, San Francisco, CA) via Dr. T. Kaneko (Department of Internal Medicine, Yokohama City University, School of Medicine, Yokohama, Japan). Cell lines A549, LC-2/ad, RERF-LC-MS, VMRC-LCD, RERF-LC-KJ, H460, and ABC-1 were gifts from Dr. Niki (Jichi Medical University, Shimotsuke, Japan). Cell lines H358, H820, and H2087 were obtained from the American Type Culture Collection (Manassas, VA), and cell line Lu65 was obtained from the Health Science Research Resources Bank (Osaka, Japan). The cells were cultured and grown in RPMI1640 (Sigma–Aldrich, St. Louis, MO) medium (H820, H2087, LC-2/ad, RERF-LC-MS, VMRC-LCD, RERF-LC-KJ, H460, H1299, Lu65, and ABC-1) or DMEM (Sigma–Aldrich) medium (16HBE14o-, A549, and H358) supplemented with 10% fetal bovine serum (Equitech-Bio, Kerrville, TX), penicillin (100 units/ml), and streptomycin (100 μg/ml) under 5% CO_2 atmosphere at 37 °C. Lung cancer tissue and corresponding normal lung tissue from a total of 51 sporadic cases of primary NSCLC were obtained from Hamamatsu University Hospital (Japan) and Seirei Mikatahara General Hospital (Japan). The tissue sample obtained from surgically resected lung was frozen in liquid nitrogen and maintained at −80 °C until used. Patients were divided into smokers and non-smokers based on their smoking history, with "non-smoker" meaning a patient who had never smoked and "smoker" meaning all others. The study design was approved by the institutional review board of both Hamamatsu University School of Medicine and Seirei Mikatahara General Hospital. A stock HU solution was prepared by dissolving HU (Sigma–Aldrich) in phosphate-buffered saline (PBS) to a concentration of 1.0 M.

2.2. Quantitative real-time (QRT)-polymerase chain reaction (PCR)

Expression of the NORE1A mRNA transcript was measured by QRT-PCR with a LightCycler instrument (Roche, Palo Alto, CA). Total RNA was extracted with an RNeasy Plus Mini Kit (QIAGEN, Valencia, CA), and 3 μg of total RNA was converted to cDNA with a SuperScript First-Strand Synthesis System for RT-PCR (Invitrogen, Carlsbad, CA). PCR amplification of the NORE1A transcript and the transcript of the control housekeeping gene *glyceraldehyde-3-phosphate dehydrogenase* (*GAPD*) was performed with the cDNA and a QuantiTect SYBR Green PCR kit (QIAGEN). The following PCR primers were used: 5′-GTG ACC TGT GCG GAC GAG AG-3′ and 5′-GGA TAA ACC CTC CTG CTG ACT GC-3′ for the NORE1A transcript and 5′-GCT CAG ACA CCA TGG GGA AG-3′ and 5′-TGT AGT TGA GGT CAA TGA AGG GG-3′ for the GAPD transcript. Although there are multiple transcripts in NORE1, the former set of PCR primers is NORE1A-specific. The relative amounts of NORE1A transcript were normalized to those of the GAPD transcript. T/N ratios were calculated by dividing the normalized transcript amounts in the cancerous tissue by the amounts in the non-cancerous tissue.

2.3. Plasmid construction

An expression vector for NORE1A (pCMV5-Flag-NORE1A) [6] was kindly provided by Dr. A.V. Khokhlatchev (Department of Pathology, University of Virginia Health Science Center, VA). NORE1A cDNA was prepared by PCR amplification by using Pfu Turbo Hotstart DNA polymerase (Stratagene, La Jolla, CA), and pCMV5-Flag-NORE1A as a template, and inserted into pEGFP-C1 vector (Clontech, Palo Alto, CA) and pcDNA3 vector (Invitrogen) to construct GFP-NORE1A expression vector and NORE1A alone expression vector, respectively. Expression vectors for L290A/I292A-type, L344A/L346A-type, and L377A/L384A-type NORE1A were generated by site-directed mutagenesis with a QuikChange Site-Directed Mutagenesis kit (Stratagene). All of the plasmid vectors were confirmed by DNA sequencing with a BigDye Terminator Cycle Sequencing Reaction Kit (Applied Biosystems, Tokyo, Japan) and an ABI 3100 Genetic Analyzer (Applied Biosystems).

2.4. Cell culture, transfection, and puromycin selection

The H1299 cells were maintained at 37 °C in RPMI1640 medium supplemented with 10% fetal bovine serum and penicillin/streptomycin under a 5% CO_2 atmosphere. A plasmid vector was transfected into the H1299 cells by using the LipofectAMINE 2000 reagent (Invitrogen) according to the supplier's recommendations. For the fluorescence *in situ* hybridization (FISH) analysis, cells were transfected with a pEGFP-C1 mammalian expression plasmid, containing or not containing NORE1A, together with a plasmid containing a puromycin resistance gene (pIRESpuro2, Clontech) at a 15:1 molar ratio. After incubation for 16 h, the medium was changed to medium containing puromycin (1.75 μg/ml). Successfully transfected cells enriched by exposure to puromycin for 40 h were then exposed to 2 mM HU for 40 h. After washing with medium, cells were cultured for an additional 72 h, and then used for the FISH analysis.

2.5. Western blot analysis

Western blot analysis using anti-NORE1A monoclonal antibody (clone 10F10, Upstate, Lake Placid, NY) or anti-β-tubulin monoclonal antibody (clone 2-28-33; Sigma–Aldrich) was performed as described previously [18].

2.6. Indirect immunofluorescence analysis

Cells were washed with PBS and fixed with methanol for 5 min at −20 °C. The cells were permeabilized with 1% Nonidet P-40 in PBS for 5 min, then incubated with 10% normal goat serum blocking solution (DAKO, Kyoto, Japan) for 30 min. The cells were then probed with mouse anti-γ-tubulin monoclonal antibody (clone GTU88; Sigma–Aldrich) at room temperature (RT) for 1 h. Indirect immunofluorescence labeling was performed by exposure to Alexa Fluor 594-conjugated goat anti-mouse IgG antibody (Molecular Probes, Eugene, OR) at RT for 1 h, and the nuclei were stained with 4′,6-diamidino-2-phenylindole (DAPI) (Sigma–Aldrich). The immunostained cells were examined under a fluorescence microscope (Olympus BX-51-FL; Olympus, Tokyo, Japan) equipped with epifluorescence filters and a photometric CCD camera (Sensicam;

PCO Company, Kelheim, Germany). The images captured were digitized and stored in the image analysis program (MetaMorph; Molecular Devices, Palo Alto, CA).

2.7. Cell proliferation assay

Cells were transfected with a pEGFP-C1 mammalian expression plasmid, containing or not containing NORE1A, together with a plasmid containing a puromycin resistance gene (pIRESpuro2, Clontech) at a 15:1 molar ratio. After puromycin selection, the cells were seeded, and the number of viable cells was counted after 24, 48, and 72 h by using a Cell Counting Kit-8 (Dojindo, Kumamoto, Japan) according to the manufacturer's instructions.

2.8. FISH analysis

FISH analysis was performed as described previously [19,29]. In brief, trypsinized cells were treated with 0.075 M KCl hypotonic solution and incubated at RT for 15 min. The cells were fixed in Carnoy's fixative twice, and the fixed cell suspension was spread onto slides over a flame. Each Spectrum Orange-labeled centromere enumeration probe (CEP; Vysis, Des Plaines, IL) solution used to identify numbers of chromosome 2 or chromosome 16 was placed on a slide and covered with a coverslip. The slides with the hybridization mixture were denatured on a digital hot plate (HP-15; AS ONE Corp., Osaka, Japan) and then incubated overnight at 42 °C. After washing the slide in 50% formamide/2× SSC, mounting medium containing DAPI (Vector Laboratories, Burlingame, CA) was used for nuclear counterstaining. The slides were promptly examined under a fluorescence microscope (Olympus BX-51-FL; Olympus) equipped with epifluorescence filters and a photometric CCD camera (Sensicam; PCO Company). The images captured were digitized and stored in the image analysis program (MetaMorph; Molecular Devices). More than 200 cells were examined in each experiment.

2.9. Statistical analysis

Data shown in the graph are means ± standard error of three experiments, and the statistical analysis was performed by using the *t*-test, chi-square test, Wilcoxon matched pairs test and JMP version 7.0.1 software (SAS Institute, Cary, NC). *p*-Values less than 0.05 were considered statistically significant.

3. Results

3.1. Down-regulation of NORE1A expression in NSCLC cell lines

We first performed a QRT-PCR analysis for NORE1A mRNA transcripts in twelve NSCLC cell lines: A549, H358, H820, H2087, LC-2/ad, RERF-LC-MS, VMRC-LCD, RERF-LC-KJ, H460, H1299, Lu65, and ABC-1. The mRNA expression levels were markedly lower in all (12/12, 100%) of the NSCLC cell lines than in immortalized human airway epithelial cell line 16HBE14o- (Fig. 1A), indicating that NORE1A mRNA expression was down-regulated in the NSCLC cell lines. Since our previous study showed that in one of the above 12 cell lines, cell line H1299, under normal growth conditions, the percentage of cells containing 3 or more centrosomes is maintained at approximately 5% [19], we considered the H1299 cell line to be suitable to use to investigate the alterations of centrosome number. We investigated the level of NORE1A protein expression in cell line H1299. The fact that the level of NORE1A mRNA expression in H1299 cells is low suggested that the NORE1A protein level would also be low, and the results of our Western blot analysis showed that the level of NORE1A protein expression in H1299 cells was below the level of detection and much lower than the level of protein expression by the 16HBE14o- cell line and normal human lung tissue (Fig. 1B). A549 cells were used as a negative control in the analysis, because previous papers have reported a low level of NORE1A protein expression in A549 cells [4,6]. We therefore decided to use H1299 cells for the NORE1A transfection experiment to investigate the role of NORE1A in centrosomes.

3.2. Centrosomal localization of NORE1A in H1299 cells

We first tried to identify the subcellular localization of N-terminally GFP-tagged NORE1A. Immunofluorescence analysis of γ-tubulin, a major centrosomal protein [10,11], in H1299 cells transfected with GFP or GFP-NORE1A expression plasmid showed that in interphase some of the GFP-NORE1A was localized at the centrosomes as well as in the nuclei and cytoplasm (Fig. 1C, middle panels), and centrosomal localization of NORE1A was also detected in the mitotic phase (Fig. 1C, lower panels). When H1299 cells were examined for cell proliferation after transfection with GFP or GFP-NORE1A plasmid together with a plasmid containing a puromycin resistance gene and puromycin selection, only a slight reduction in growth was detected in the enriched GFP-NORE1A-transfected lung cancer cells compared with the GFP transfected cells (Fig. 1D), which is consistent with a previous report [6].

3.3. NORE1A suppresses the centrosome amplification induced by HU

When some cell lines have been exposed to the DNA synthesis inhibitor HU, the centrosomes continue to reduplicate, resulting in the generation of amplified centrosomes [13,16,30]. We therefore attempted to determine the effect of NORE1A on the regulation of centrosome number in cells exposed to HU. First, we exposed H1299 cells to HU for 40 h and counted the number of centrosomes they contained by immunofluorescence analysis with anti-γ-tubulin antibody. The results showed a significantly higher frequency of cells containing 3 or more centrosomes was among the HU-exposed cells than among the control cells (Fig. 2A), meaning that centrosome amplification had been induced in the cells exposed to HU. Next, we transfected H1299 cells with the GFP-NORE1A or control GFP expression plasmid and exposed them to HU for 40 h. Forced expression of NORE1A had no clear effect on the control cells, but resulted in a significant reduction in the frequency of HU-exposed cells containing 3 or more centrosomes (Fig. 2B), suggesting that NORE1A has activity that partially suppresses the centrosome amplification induced by HU.

3.4. Wild-type (Wt) NORE1A, but not NES-mutant NORE1A, suppresses the centrosome amplification induced by HU

Since NORE1A is a nucleocytoplasmic shuttling protein [8], the nuclear export signal (NES) may be present in NORE1A protein. Because the centrosomes are located in the cytoplasm [12,13], we investigated whether the NES mutation abrogates the ability of NORE1A to localize to centrosomes and control the numerical integrity of centrosomes. When the amino acid sequence of NORE1A was screened with the NES predictor program NetNES [31], three regions were suspected of a leucine-rich NES. We introduced point mutations to each putative NES and constructed GFP-NORE1A-L290A/I292A, -L344A/L346A, and -L377A/L384A expression plasmids, and Western blot analysis confirmed that all three GFP-NORE1A proteins were expressed at a similar molecular size (Fig. 2C). Then, their subcellular localization was investigated by examining the cells with a fluorescence microscope, and localization of NORE1A-wt, -L290A/I292A, and -L344A/L346A was observed in both the nucleus and cytoplasm, whereas NORE1A-L377A/L384A was localized in

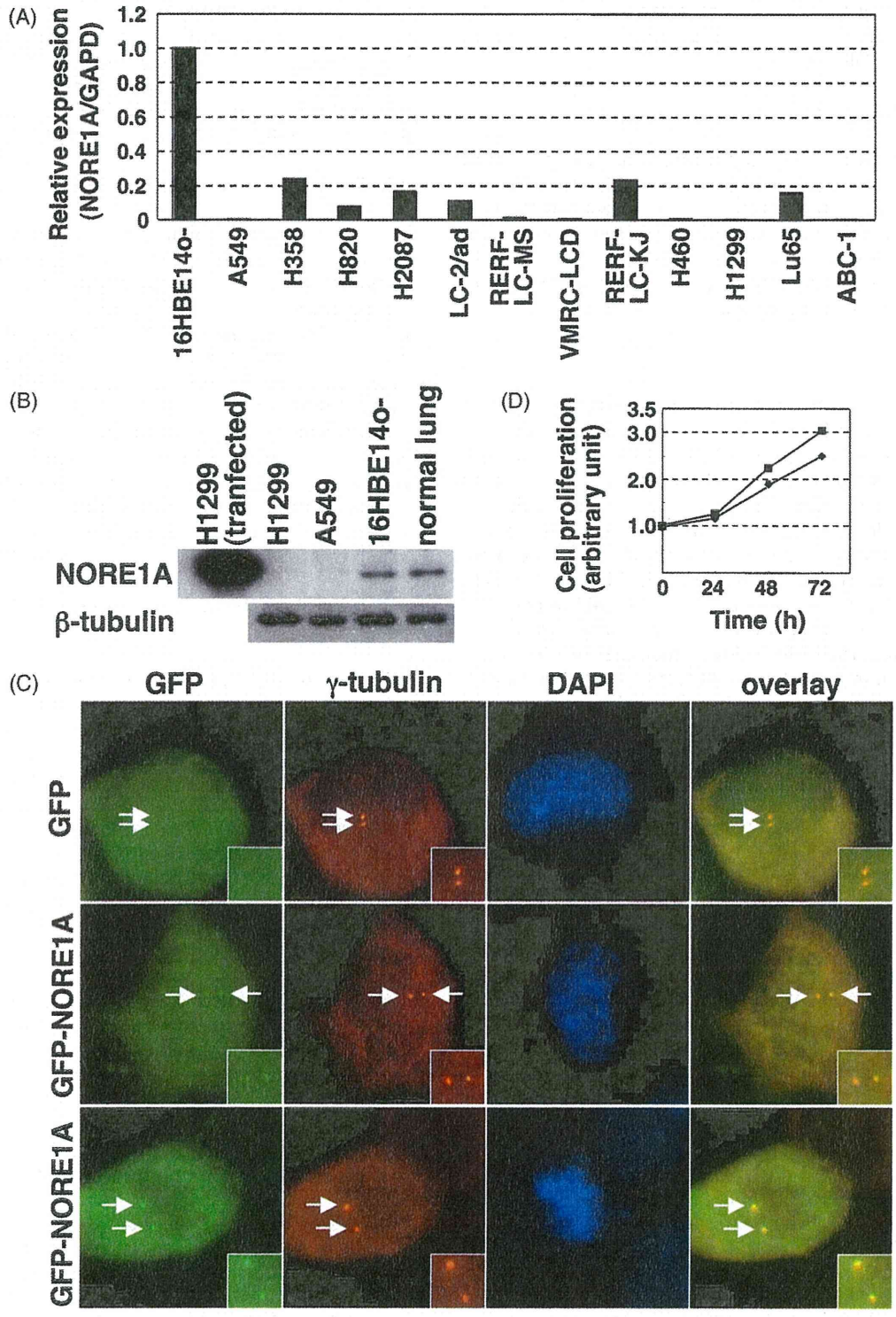

Fig. 1. Down-regulation of NORE1A expression in non-small cell lung carcinoma (NSCLC) cell lines and centrosomal localization of NORE1A. (A) Measurement of the level of expression of NORE1A transcripts in NSCLC cell lines by quantitative real-time-polymerase chain reaction with a LightCycler instrument. The amounts of NORE1A transcripts normalized to the amount of transcripts of a housekeeping gene, *GAPD*, in 12 NSCLC cell lines are shown in the graph. The NORE1A expression level of human airway epithelial cell line 16HBE14o- was measured as a control and set equal to 1.0. (B) Measurement of the level of NORE1A protein expression in cell lines H1299 and A549 NSCLC by Western blot analysis with anti-NORE1A monoclonal antibody. H1299 cells transiently transfected with NORE1A expression vector, human airway epithelial cell line 16HBE14o-, and human non-cancerous lung tissue were also used. A smaller amount of total cell extract was applied in the NORE1A-transfected H1299 cell lane for SDS-PAGE than in the other lanes. Expression of β-tubulin protein was analyzed as an internal control. (C) Detection of the subcellular localization of NORE1A in H1299 cells. H1299 cells transiently transfected with GFP or GFP-NORE1A expression vector (green) and then immunostained with mouse anti-γ-tubulin monoclonal antibody (red). Nuclei were stained with DAPI (blue). Representative immunostaining images are shown. Arrows point to the positions of centrosomes. The upper and middle panels show interphase cells, and the lower panels show mitotic phase cells. (D) Proliferation of H1299 cells transfected with GFP vector (squares) or GFP-NORE1A expression vector (diamonds). Cell numbers were counted by using a Cell Counting Kit-8.

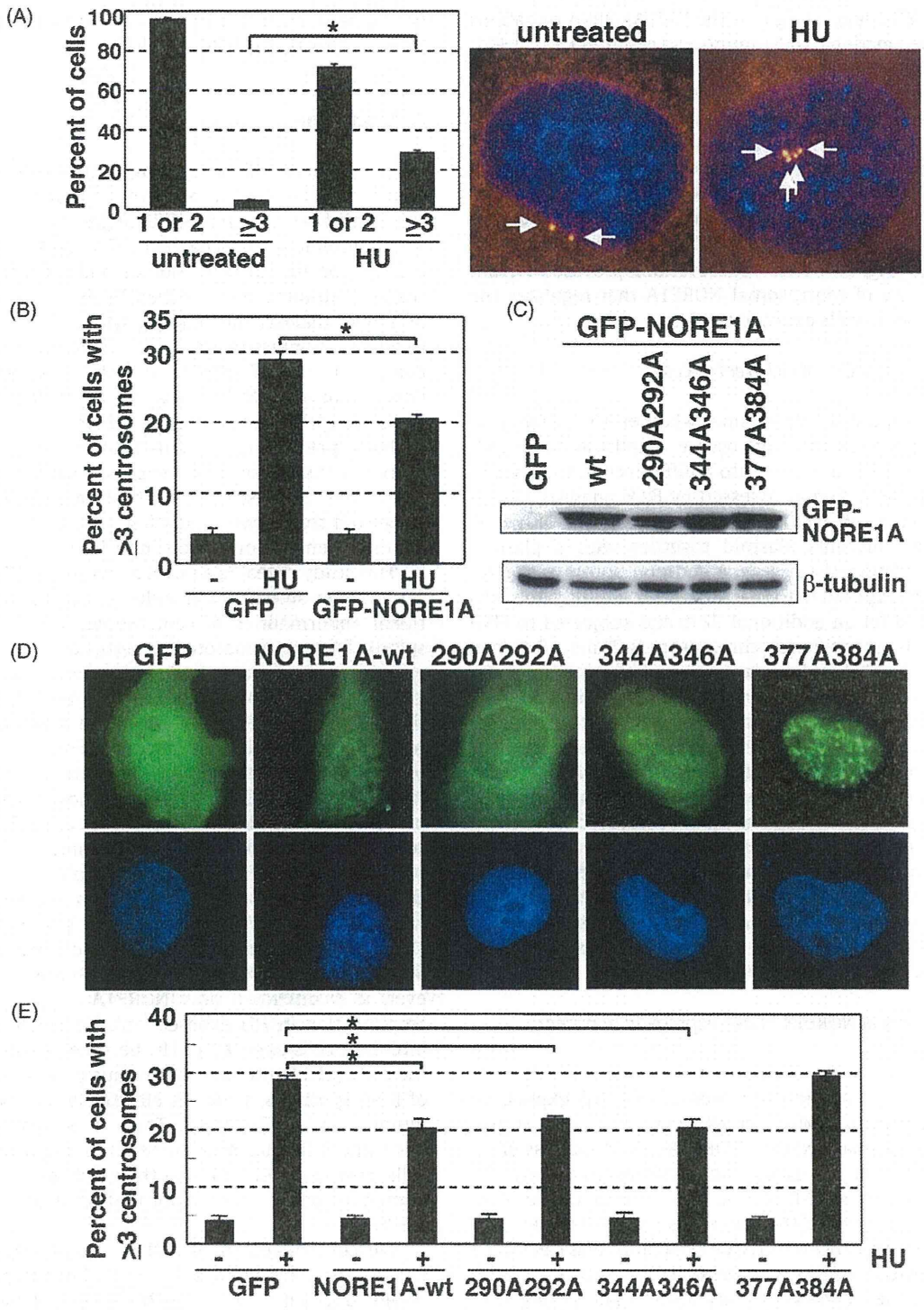

Fig. 2. Wild-type (wt) NORE1A, but not nuclear export signal (NES)-mutant NORE1A, suppresses centrosome amplification induced by hydroxyurea (HU). (A) Induction of centrosome amplification in H1299 cells as a result of HU exposure. H1299 cells were exposed or not exposed to HU for 40 h, and then immunostained with mouse anti-γ-tubulin monoclonal antibody (red). Nuclei were stained with DAPI (blue). The number of centrosomes per cell was counted, and the counts are shown in the left panel. A *t*-test was performed for statistical analysis and an asterisk in the graph indicates a statistically significant difference. Representative immunostaining images are shown in the right panels. Arrows indicate the centrosomes. (B) NORE1A suppresses centrosome amplification induced by HU. H1299 cells were transiently transfected with GFP-NORE1A or GFP expression plasmid, and 18 h later, the cells were exposed or not exposed to HU for 40 h, and then immunostained with mouse anti-γ-tubulin antibody. The percentages of cells containing 3 or more centrosomes were calculated. A *t*-test was performed for statistical analysis and an asterisk in the graph indicates a statistically significant difference. (C) Expression of the wt form and putative NES mutant forms of GFP-NORE1A proteins detected by Western blot analysis with anti-NORE1A monoclonal antibody. H1299 cells were transiently transfected with GFP-NORE1A expression vectors and examined for NORE1A expression. Expression of β-tubulin protein was analyzed as an internal control. (D) Subcellular localization of the wt form and putative NES mutant forms of GFP-NORE1A proteins in H1299 cells. H1299 cells were transiently transfected with GFP or GFP-NORE1A expression vectors (green), and then examined for their localization under a fluorescence microscope. Nuclei were stained with DAPI (blue). Representative immunostaining images are shown. (E) NORE1A-L377A/L384A does not suppress centrosome amplification induced by HU. H1299 cells were transiently transfected with the wt form and putative NES mutant forms of GFP-NORE1A or GFP expression plasmid, and 18 h after transfection, the cells were exposed to HU for 40 h or not exposed, and then immunostained with mouse anti-γ-tubulin antibody. The percentages of cells containing 3 or more centrosomes were determined. A *t*-test was performed for statistical analysis and an asterisk in the graph indicates a statistically significant difference.

the nucleus (Fig. 2D), suggesting that the L377A/L384A mutations had destroyed the functional NES (amino acid residues L377–L384) of NORE1A. Next, we transfected H1299 cells with the one of the GFP-NORE1A plasmids or control GFP expression plasmid and exposed them to HU for 40 h. Determination of centrosome number in these cells after immunofluorescence analysis with anti-γ-tubulin antibody revealed that two of mutants, NORE1A-L290A/I292A and -L344A/L346A, as well as NORE1A-wt had activity that significantly suppressed the centrosome amplification induced by HU, but that the NORE1A-L377A/L384A mutant did not possess such activity (Fig. 2E). These observations provided further evidence for activity of centrosomal NORE1A that regulates the centrosome number in cells exposed to HU.

3.5. *NORE1A suppresses CIN in HU-treated cells*

Next, we attempted to determine whether the activity of NORE1A that suppresses the centrosome amplification in HU-exposed H1299 cells is translated into a difference in the level of chromosome destabilization as assessed by FISH analysis. H1299 cells were transfected with GFP, GFP-NORE1A-wt, or GFP-NORE1A-L377A/L384A (NES mutant) plasmid together with a plasmid containing a puromycin resistance gene, and after puromycin selection, the cells were exposed to HU for 40 h. After washing, the cells were then cultured for an additional 72 h, and subjected to FISH analysis with probes specific for chromosomes 2 and 16. When the cells were divided according to number of chromosomes per cell into cells containing the modal chromosome number and cells containing other chromosome numbers, cells containing the modal chromosome number were found to be significantly less frequent among the HU-exposed cells than among the control cells (Fig. 3A; Fig. 3B shows representative images). Importantly, comparison of the frequency of cells containing the modal chromosome number among HU-exposed cells showed that it was significantly higher among the cells transfected with the GFP-NORE1A-wt expression vector, but not with the GFP-NORE1A-L377A/L384A expression vector, than among cells transfected with the GFP vector (Fig. 3A and B), suggesting that wt NORE1A, but not NES-mutant NORE1A, suppresses CIN in HU-exposed H1299 cells.

3.6. *Down-regulation of NORE1A mRNA expression in primary NSCLC*

Next, to better understand the status of NORE1A expression in NSCLC, we investigated whether NORE1A expression is also down-regulated in primary NSCLC. NORE1A mRNA expression in 51 primary NSCLC and corresponding non-cancerous lung tissues was measured by QRT-PCR, and the ratio of the level of NORE1A mRNA expression in the cancerous tissue to the level in the corresponding non-cancerous tissue (T/N ratio) was calculated in each case. Reduced NORE1A expression (T/N ratio < 0.5) was observed in 25 of the 51 (49%) primary NSCLC cancers (Fig. 4A). Moreover, a significant difference was detected in the NORE1A expression level between cancerous tissue and the corresponding non-cancerous tissue by a statistical analysis (p-value = 0.013 by Wilcoxon matched pairs test). Reduced NORE1A protein expression in the cancerous tissue compared with the corresponding non-cancerous tissue was detected in two cases showing reduced NORE1A mRNA expression by Western blot analysis (Fig. 4B). These results suggest that NORE1A mRNA expression is down-regulated in primary NSCLCs. Finally, we investigated whether the levels of NORE1A mRNA expression were associated with clinicopathological features in NSCLC patients. Although no associations were found between the clinicopathological factors onset age, smoking history, tumor stage, or tumor histology and the NORE1A mRNA expression levels, the frequency of male patients was higher in the group of NSCLC patients with a T/N ratio < 1 than in the group with a T/N ratio ≥ 1 (p-value = 0.006) (Table 1).

4. Discussion

The results of this study showed that exposure of H1299 NSCLC cells to HU resulted in abnormal centrosome amplification and that forced expression of NORE1A partially suppressed the centrosome amplification. NORE1A-L377A/L384A, an NES mutant form, did not localize to centrosomes and did not suppress the centrosome amplification induced by HU. Furthermore, the results of a FISH analysis showed that wt NORE1A, but not NES-mutant NORE1A, suppressed CIN in HU-exposed H1299 cells. Next, we compared level of NORE1A mRNA expression in the cancerous tissue of primary NSCLCs and corresponding non-cancerous lung tissue by QRT-PCR analysis, and the results showed that NORE1A mRNA expression was down-regulated in 25 (49%) of the 51 primary NSCLCs. These results suggest that NORE1A has activity that suppresses centrosome amplification induced by HU, and they suggested that down-regulation of NORE1A mRNA is one of the common gene abnormalities in NSCLCs.

This study revealed a novel activity of NORE1A that suppresses centrosome amplification induced by HU. Numerical and functional abnormalities of centrosomes result in aberrant mitotic spindle formation, merotelic kinetochore-microtubule attachment errors, lagging chromosome formation, and chromosome segregation errors, all of which are thought to be possible causes of CIN [12–15]. Many cancer-associated proteins have already been reported to be involved in controlling the numerical integrity of centrosomes, centrosome duplication, and centrosome function/behavior [13]. Interestingly, most such cancer-associated proteins are localized at centrosomes [12,13]. For example, tumor suppressor p53 is involved in the control of numerical integrity of centrosomes [13,18,30,32]. The p53 is a nucleocytoplasmic shuttling protein and some p53 is localized at centrosomes [13,18,30,32–34]. We therefore think that it is reasonable to conclude NORE1A, some of which is localized at centrosomes, has activity that controls the numerical integrity of centrosomes. However, it is unknown how NORE1A suppresses the centrosome amplification in HU-exposed cells. Since HU is a DNA synthesis inhibitor, cells exposed to HU become arrested in the S-phase of the cell cycle. Centrosomes continue to reduplicate in the absence of DNA synthesis, which is effectively observed if *p53* is lost or mutated [13,16–20,30,32]. Thus, it is speculated that NORE1A has some influence on centrosome reduplication in HU-arrested cells. Future investigation of the mechanism underlying the phenomenon should improve our understanding of carcinogenesis in the lung.

We constructed three NORE1A expression plasmids, each of which contains mutations in the NES region predicted by NetNES server [31], but only the NORE1A-L377A/L384A expression plasmid failed to exhibit cytoplasmic localization, suggesting that the leucine-rich amino acid residues L377–L384 (LQNFLTIL) of NORE1A are a functional NES. Park et al. also showed that this NES sequence is functional [8]. Interestingly, comparison of the amino acid sequences of NORE1A orthologues has shown that the NES region is conserved among *Homo sapiens*, *Mus musculus*, *Rattus norvegicus*, and *Bos taurus*. Since the cytoplasmic localization of NORE1A is essential for its growth-suppressive activity [6] and abrogation of nuclear export results in failure to suppress centrosome amplification as shown in this study, the NES sequence of NORE1A must be important in achieving these functions.

The FISH analysis (Fig. 3) of HU-exposed cells in our study showed a significantly higher proportion of cells containing the modal chromosome number among the cells transfected with the

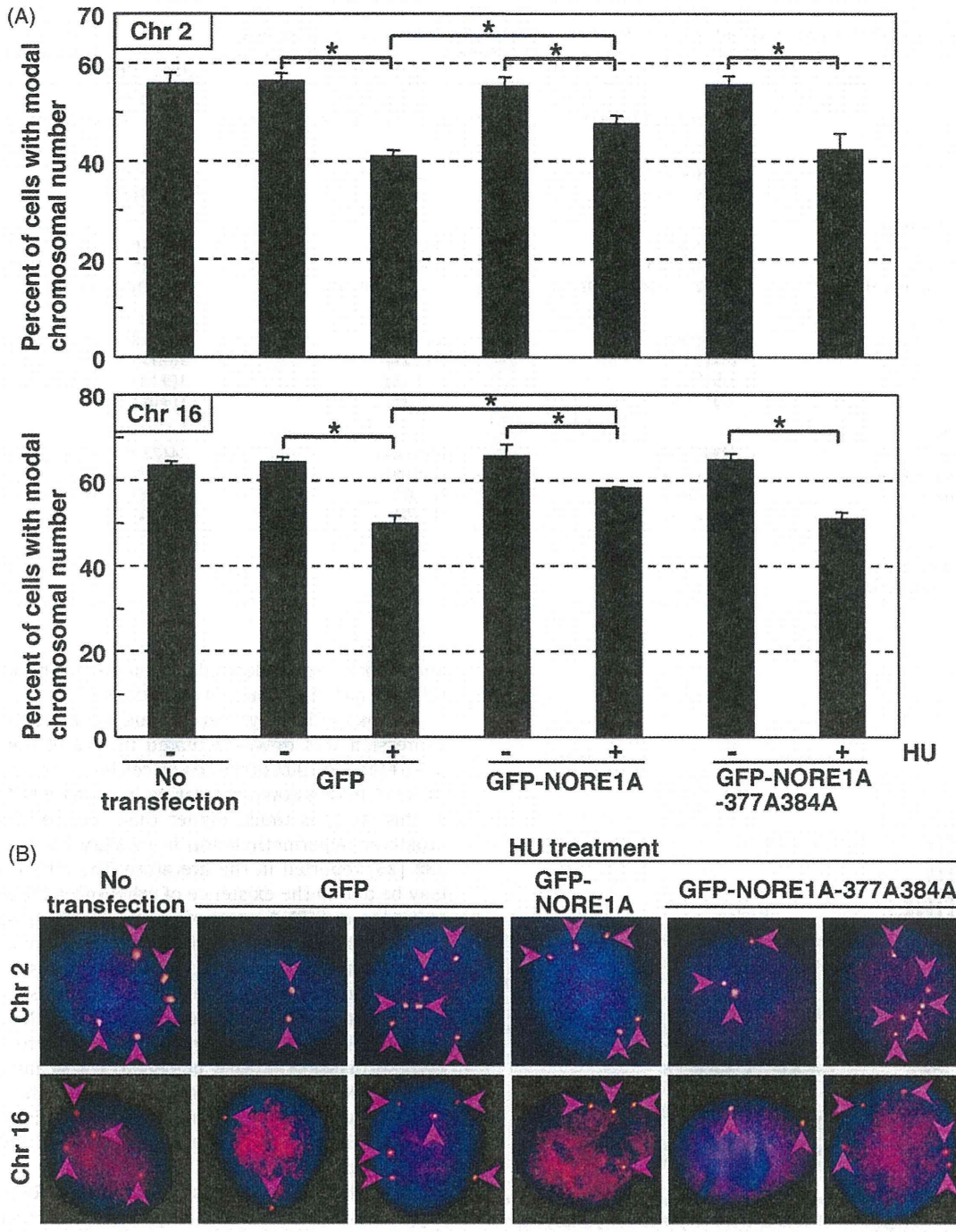

Fig. 3. Wild-type (wt) NORE1A, but not nuclear export signal (NES)-mutant NORE1A, suppresses chromosome instability in hydroxyurea (HU)-exposed H1299 cells. (A and B) H1299 cells were transiently transfected with GFP, GFP-NORE1A-wt, or GFP-NORE1A-L377A/L384A plasmid together with a plasmid containing a puromycin resistance gene, and 40 h later, the cells were exposed to HU for 40 h. The cells were then replated in fresh medium, cultured for an additional 72 h, and subjected to FISH analysis with a Spectrum Orange-labeled centromere enumeration probe. Nuclei were stained with DAPI (blue). The percentages of cells containing the modal chromosome number are shown in the upper panel (chromosome 2) and the lower panel (chromosome 16) of (A). A *t*-test was performed for statistical analysis and an asterisk in the graph indicates a statistically significant difference. Representative images of the results of the FISH analysis are shown in (B). Arrows point to the chromosomes.

GFP-NORE1A-wt expression vector than among the cells transfected with the GFP vector, however, the increase was modest. The fact that the increase was modest is thought to have been due to one of the following possible limitations of this study: (1) HU was not able to induce CIN effectively under the conditions used in our experiment, (2) the use of transiently transfected cells, not stably transfected cells, (3) the H1299 cell line was unsuitable for detecting a clear inhibitory effect of NORE1A on CIN, and (4) chromosomes 2 and 16 were unsuitable for detecting a clear inhibitory effect of NORE1A on CIN.

The cell proliferation analysis in our study revealed that NORE1A has a slight effect on growth suppression in H1299 cells growing as a monolayer on plastic. Two studies on the growth-suppressive function of NORE1A in NSCLC cell lines have been reported [5,6]. In the study by Moshnikova et al. [6] forced expression of NORE1A was found to inhibit anchorage-independent growth of A549 NSCLC cells, but not to affect anchorage-dependent growth of the cells. Aoyama et al. [5] also reported finding that forced expression of NORE1A markedly suppressed anchorage-independent growth of A549 cells, however, they found that under

Table 1
Clinicopathological factors of NSCLC patients according to the T/N ratio of the NORE1A mRNA expression in their lung.

Factor	Total (n = 51)	T/N ≥ 1 (n = 18)	T/N < 1 (n = 33)	p-Value
Age (51 cases)				
Mean ± SD[a]	65.1 ± 12.8 (n = 51)	63.4 ± 13.9 (n = 18)	66.1 ± 12.3 (n = 33)	0.491[b]
Gender (51 cases)				
Male	30 (60.1%)	6 (33.3%)	24 (72.7%)	0.006[c]
Female	21 (39.9%)	12 (66.7%)	9 (27.3%)	
Smoking history (40 cases)				
Smoker	29 (65.2%)	7 (63.6%)	22 (75.9%)	0.447[c]
Non-smoker	11 (34.8%)	4 (36.4%)	7 (24.1%)	
Brinkman index (mean ± SD)	872 ± 1034 (n = 40)	889 ± 973 (n = 11)	866 ± 1072 (n = 29)	0.952[b]
Tumor stage (51 cases)				
I	36 (70.6%)	10 (55.6%)	26 (78.8%)	0.311[c]
II	7 (13.7%)	4 (22.2%)	3 (9.1%)	
III	5 (9.8%)	2 (11.1%)	3 (9.1%)	
IV	3 (5.9%)	2 (11.1%)	1 (3.0%)	
Histology (51 cases)				
Adenocarcinoma	34 (66.7%)	10 (55.6%)	24 (72.7%)	0.231[c]
Squamous cell carcinoma	15 (29.4%)	7 (38.9%)	8 (24.2%)	
Large cell carcinoma	1 (2.0%)	0 (0.0%)	1 (3.0%)	
Adenosquamous carcinoma	1 (2.0%)	1 (5.6%)	0 (0.0%)	

[a] SD, standard deviation.
[b] A t-test was performed.
[c] A chi-square test was performed.

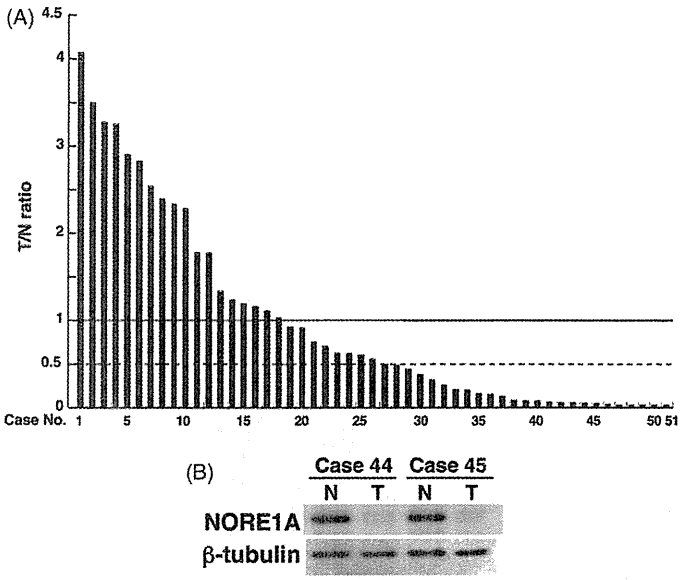

Fig. 4. Down-regulation of NORE1A expression in primary non-small cell lung carcinoma (NSCLC). (A) Down-regulation of NORE1A mRNA expression in primary NSCLC. Comparison between the NORE1A mRNA level in cancerous tissue of 51 primary NSCLCs and corresponding non-cancerous lung tissue as determined by quantitative real-time-polymerase chain reaction analysis. After normalizing the amounts of NORE1A transcripts to those of the GAPD transcript, T/N values were calculated by dividing the amount of normalized transcripts in cancerous tissue by the amount in the corresponding non-cancerous tissue. Differences between the normalized NORE1A mRNA level in cancerous tissue and corresponding non-cancerous tissue were statistically analyzed by the Wilcoxon matched pairs test, and the p-value was 0.013. (B) Down-regulation of NORE1A protein expression in primary NSCLC. Measurement of the level of NORE1A protein expression in cancerous tissue (T) and corresponding non-cancerous tissue (N) by Western blot analysis with anti-NORE1A monoclonal antibody in two NSCLC cases. Expression of β-tubulin protein was analyzed as an internal control.

anchorage-dependent growth conditions NORE1A expression suppressed colony formation by A549 and H460 NSCLC cells by 73% and 23%, respectively. Thus, the growth-suppressive effect of NORE1A under anchorage-dependent conditions seems to be weaker than under anchorage-independent conditions and may vary with the cell type and experimental conditions.

The QRT-PCR analysis in our study revealed that NORE1A mRNA expression was down-regulated in 49% of the primary NSCLCs (n = 51) and in 100% of the NSCLC cell lines (n = 12). The frequency of NORE1A mRNA down-regulation in primary NSCLCs of 49% found in this study is much higher than the frequencies of NORE1A promoter hypermethylation in primary NSCLCs of 24% [22] and 28% [23] reported in the literature. The differences in frequency may be due to the existence of other mechanisms underlying the reduction of mRNA expression level, such as histone deacetylation, microRNA abnormalities, and allelic imbalance [24–26,35]. The results of the expression analysis in this study also showed an association between male NSCLC patients and a reduction of NORE1A expression in the cancerous tissue (T/N ratio < 1). Although the reason for this association is unknown, there are sex differences in the expression of other genes [36,37]. In any event, the results of the mRNA expression analysis suggested that down-regulation of NORE1A mRNA is a common abnormality in the carcinogenesis of NSCLC, the same as down-regulation of p16, RASSF1A, and CDH1 expressions [38,39].

In conclusion, our results suggest that NORE1A has activity that suppresses the centrosome amplification induced by HU and that NORE1A mRNA down-regulation is one of the common gene abnormalities in NSCLCs. These imply a key preventive role of NORE1A against the carcinogenesis of NSCLC.

Conflicts of interest

None declared.

Acknowledgements

We are grateful to Dr. A.V. Khokhlatchev (University of Virginia Health Science Center, VA) for providing us with pCMV5-Flag-NORE1A plasmid vector. We are also grateful to Dr. D.C. Gruenert (California Pacific Medical Center Research Institute, CA) and Dr. T. Kaneko (Yokohama City University, School of Medicine, Japan) for providing us with 16HBE14o- cell line and to Dr. T. Niki (Jichi

Medical University, Japan) for providing us with 7 lung cancer cell lines. We acknowledge Mr. T. Kamo (Hamamatsu University School of Medicine) for his technical assistance. MG is a Center of Excellence research assistant in Hamamatsu Univ Sch Med. This work was supported by grants from the Ministry of Health, Labour and Welfare (19–19), the Japan Society for the Promotion of Science (19790286), the Ministry of Education, Culture, Sports, Science and Technology (20014007), the 21st Century COE program, and the Smoking Research Foundation.

References

[1] Vavvas D, Li X, Avruch J, Zhang XF. Identification of Nore1 as a potential Ras effector. J Biol Chem 1998;273:5439–42.
[2] Tommasi S, Dammann R, Jin SG, Zhang XF, Avruch J, Pfeifer GP. RASSF3 and NORE1: identification and cloning of two human homologues of the putative tumor suppressor gene RASSF1. Oncogene 2002;21:2713–20.
[3] Nakamura N, Carney JA, Jin L, Kajita S, Pallares J, Zhang H, et al. RASSF1A and NORE1A methylation and BRAFV600E mutations in thyroid tumor. Lab Invest 2005;85:1065–75.
[4] Vos MD, Martinez A, Ellis CA, Vallecorsa T, Clark GJ. The pro-apoptotic Ras effector Nore1 may serve as a Ras-regulated tumor suppressor in the lung. J Biol Chem 2003;278:21938–43.
[5] Aoyama Y, Avruch J, Zhang XF. Nore1 inhibits tumor cell growth independent of Ras or the MST1/2 kinases. Oncogene 2004;23:3426–33.
[6] Moshnikova A, Frye J, Shay JW, Minna JD, Khokhlatchev AV. The growth and tumor suppressor NORE1A is a cytoskeletal protein that suppresses growth by inhibition of the ERK pathway. J Biol Chem 2006;281:8143–52.
[7] Moshnikova A, Kuznetsov S, Khokhlatchev AV. Interaction of the growth and tumour suppressor NORE1A with microtubules is not required for its growth-suppressive function. BMC Res Notes 2008;1:1–7.
[8] Park SJ, Lee D, Choi CY, Ryu SY. Induction of apoptosis by NORE1A in a manner dependent on its nuclear export. Biochem Biophys Res Commun 2008;368:56–61.
[9] Calvisi DF, Donninger H, Vos MD, Birrer MJ, Gordon L, Leaner V, et al. NORE1A tumor suppressor candidate modulates p21CIP1 via p53. Cancer Res 2009;69:4629–37.
[10] Joshi HC. Microtubule organizing centers and gamma-tubulin. Curr Opin Cell Biol 1994;6:54–62.
[11] Oakley BR. Gamma-tubulin. Curr Top Dev Biol 2000;49:27–54.
[12] Nigg EA. Centrosome aberrations: cause or consequence of cancer progression? Nat Rev Cancer 2002;2:815–25.
[13] Fukasawa K. Oncogenes and tumour suppressors take on centrosomes. Nat Rev Cancer 2007;7:911–24.
[14] Lingle WL, Barrett SL, Negron VC, D'Assoro AB, Boeneman K, Liu W, et al. Centrosome amplification drives chromosomal instability in breast tumor development. Proc Natl Acad Sci USA 2002;99:1978–83.
[15] Ganem NJ, Godinho SA, Pellman D. A mechanism linking extra centrosomes to chromosomal instability. Nature 2009;460:278–82.
[16] Balczon R, Bao L, Zimmer WE, Brown K, Zinkowski RP, Brinkley BR. Dissociation of centrosome replication events from cycles of DNA synthesis and mitotic division in hydroxyurea-arrested Chinese hamster ovary cells. J Cell Biol 1995;130:105–15.
[17] Tarapore P, Horn HF, Tokuyama Y, Fukasawa K. Direct regulation of the centrosome duplication cycle by the p53-p21Waf1/Cip1 pathway. Oncogene 2001;20:3173–84.
[18] Shinmura K, Bennett RA, Tarapore P, Fukasawa K. Direct evidence for the role of centrosomally localized p53 in the regulation of centrosome duplication. Oncogene 2007;26:2939–44.
[19] Shinmura K, Iwaizumi M, Igarashi H, Nagura K, Yamada H, Suzuki M, et al. Induction of centrosome amplification and chromosome instability in p53-deficient lung cancer cells exposed to benzo[a]pyrene diol epoxide (B[a]PDE). J Pathol 2008;216:365–74.
[20] Dodson H, Bourke E, Jeffers LJ, Vagnarelli P, Sonoda E, Takeda S, et al. Centrosome amplification induced by DNA damage occurs during a prolonged G2 phase and involves ATM. EMBO J 2004;23:3864–73.
[21] Destro A, Ceresoli GL, Baryshnikova E, Garassino I, Zucali PA, De Vincenzo F, et al. Gene methylation in pleural mesothelioma: correlations with clinicopathological features and patient's follow-up. Lung Cancer 2008;59:369–76.
[22] Hesson L, Dallol A, Minna JD, Maher ER, Latif F. NORE1A, a homologue of RASSF1A tumour suppressor gene is inactivated in human cancers. Oncogene 2003;22:947–54.
[23] Irimia M, Fraga MF, Sanchez-Cespedes M, Esteller M. CpG island promoter hypermethylation of the Ras-effector gene NORE1A occurs in the context of a wild-type K-ras in lung cancer. Oncogene 2004;23:8695–9.
[24] Peinado H, Ballestar E, Esteller M, Cano A. Snail mediates E-cadherin repression by the recruitment of the Sin3A/histone deacetylase 1 (HDAC1)/HDAC2 complex. Mol Cell Biol 2004;24:306–19.
[25] Esteller M. Epigenetics in cancer. N Engl J Med 2008;358:1148–59.
[26] Croce CM. Causes and consequences of microRNA dysregulation in cancer. Nat Rev Genet 2009;10:704–14.
[27] Masuda A, Takahashi T. Chromosome instability in human lung cancers: possible underlying mechanisms and potential consequences in the pathogenesis. Oncogene 2002;21:6884–97.
[28] Cozens AL, Yezzi MJ, Kunzelmann K, Ohrui T, Chin L, Eng K, et al. CFTR expression and chloride secretion in polarized immortal human bronchial epithelial cells. Am J Respir Cell Mol Biol 1994;10:38–47.
[29] Kitayama Y, Igarashi H, Watanabe F, Maruyama Y, Kanamori M, Sugimura H. Nonrandom chromosomal numerical abnormality predicting prognosis of gastric cancer: a retrospective study of 51 cases using pathology archives. Lab Invest 2003;83:1311–20.
[30] Ma Z, Izumi H, Kanai M, Kabuyama Y, Ahn NG, Fukasawa K. Mortalin controls centrosome duplication via modulating centrosomal localization of p53. Oncogene 2006;25:5377–90.
[31] la Cour T, Kiemer L, Mølgaard A, Gupta R, Skriver K, Brunak S. Analysis and prediction of leucine-rich nuclear export signals. Protein Eng Des Sel 2004;17:527–36.
[32] Tarapore P, Fukasawa K. Loss of p53 and centrosome hyperamplification. Oncogene 2002;21:6234–40.
[33] Blair Zajdel ME, Blair GE. The intracellular distribution of the transformation-associated protein p53 in adenovirus-transformed rodent cells. Oncogene 1988;2:579–84.
[34] Brown CR, Doxsey SJ, White E, Welch WJ. Both viral (adenovirus E1B) and cellular (hsp70, p53) components interact with centrosomes. J Cell Physiol 1994;160:47–60.
[35] Toma MI, Grosser M, Herr A, Aust DE, Meye A, Hoefling C, et al. Loss of heterozygosity and copy number abnormality in clear cell renal cell carcinoma discovered by high-density affymetrix 10K single nucleotide polymorphism mapping array. Neoplasia 2008;10:634–42.
[36] Mollerup S, Ryberg D, Hewer A, Phillips DH, Haugen A. Sex differences in lung CYP1A1 expression and DNA adduct levels among lung cancer patients. Cancer Res 1999;59:3317–20.
[37] Merino G, van Herwaarden AE, Wagenaar E, Jonker JW, Schinkel AH. Sex-dependent expression and activity of the ATP-binding cassette transporter breast cancer resistance protein (BCRP/ABCG2) in liver. Mol Pharmacol 2005;67:1765–71.
[38] Yokota J, Kohno T. Molecular footprints of human lung cancer progression. Cancer Sci 2004;95:197–204.
[39] Topaloglu O, Hoque MO, Tokumaru Y, Lee J, Ratovitski E, Sidransky D, et al. Detection of promoter hypermethylation of multiple genes in the tumor and bronchoalveolar lavage of patients with lung cancer. Clin Cancer Res 2004;10:2284–8.

EML4-ALK fusion transcripts in immunohistochemically ALK-positive non-small cell lung carcinomas

KAZUYA SHINMURA[1], SHINJI KAGEYAMA[1], HISAKI IGARASHI[1], TAKAHARU KAMO[1], TAKAHIRO MOCHIZUKI[2], KAZUYA SUZUKI[2], MASAYUKI TANAHASHI[3], HIROSHI NIWA[3], HIROSHI OGAWA[4] and HARUHIKO SUGIMURA[1]

[1]First Department of Pathology, and [2]First Department of Surgery, Hamamatsu University School of Medicine, Hamamatsu 431-3192; [3]Division of Thoracic Surgery, Respiratory Disease Center, and [4]Division of Pathology, Seirei Mikatahara General Hospital, Hamamatsu 433-8558, Japan

Received October 12, 2009; Accepted November 27, 2009

DOI: 10.3892/etm_00000042

Abstract. EML4-ALK fusion transcripts have been found in a subset of non-small cell lung carcinomas (NSCLCs); however, their protein expression status has not yet been fully elucidated. In this study we investigated ALK protein expression in 302 NSCLCs and 291 gastric carcinomas by means of immunohistochemical analysis. Twelve (4.0%) NSCLCs, but none of the gastric carcinomas, were found to be positive for ALK. The ALK signal was detected in the cytoplasm of cancer cells. Subsequent RNA analysis of 10 RNA-available, immunohistochemically ALK-positive tumors revealed that three tumors had EML4-ALK variant 1, three tumors had variant 2, three tumors had variants 3a and 3b, and one tumor had a novel variant in which exon 14 of EML4 is connected to the nucleotide at position 53 of exon 20 of ALK by a 2-bp insertion. These results suggest that immunohistochemical ALK detection is a useful way to screen NSCLCs for tumors containing ALK fusions.

Introduction

Structural chromosome aberrations that result in the production of fusion oncogenes are one of the most common causes of oncogenesis. In the past they have been reported in many classes of hematological malignancies and mesenchymal tumors (1,2), and recently in a few types of epithelial carcinomas (3-5). A fusion gene comprising portions of the *EML4* gene and the *ALK* gene that resulted from a small inversion in chromosome 2p was recently discovered in a subset of non-small cell lung carcinomas (NSCLCs) (4). The fused mRNA based on the gene fusion encodes the N-terminal portion of EML4 ligated to the intracellular region of the receptor-type protein tyrosine kinase ALK. EML4-ALK oligomerizes constitutively in cells through the coiled-coil domain within the EML4 region and becomes activated to exert oncogenicity both *in vitro* and *in vivo* (4,6). Several types of EML4-ALK variants have been found in NSCLCs (4,6-18), and although one NSCLC containing KIF5B-ALK and another NSCLC containing TFG-ALK have been found (13,15), all of the other ALK fusions detected in NSCLCs have been EML4-ALK fusions.

Notably, recent studies have shown that ALK inhibitors have potential therapeutic efficacy for NSCLCs that are positive for ALK fusion proteins (4,6,16,19). Thus, the development of a diagnostic system for NSCLCs expressing ALK fusion proteins will be essential to identifying subgroups of NSCLC patients for treatment with ALK inhibitors. Immunohistochemical analysis of paraffin-embedded sections during routine pathologic diagnosis is a convenient means of examining the level of protein expression when the analytical condition is determined. Takeuchi *et al* recently reported an effective means of immunohistochemical detection of EML4-ALK by the intercalated antibody-enhanced polymer (iAEP) method (13). However, another group reported difficulty detecting EML4-ALK immunohistochemically (14), and it is speculated that the low expression level of EML4-ALK protein may be attributable to a low level of EML4 transcriptional activity or to instability of EML4-ALK in cells (13). Moreover, based on the results of a fluorescence *in situ* hybridization (FISH) analysis, Perner *et al* reported finding that only a subset of tumor cells contains the 2p rearrangement that leads to the formation of EML4-ALK (10). Thus, a system for immunohistochemical detection of ALK in NSCLCs would need to be established in order to diagnose tumors containing ALK fusions and elucidate the expression status of ALK fusion proteins. We also believe that immunohistochemical screening for ALK fusions may lead to the identification of novel EML4-ALK variants or novel fusions with ALK in addition to known EML4-ALK variants. Moreover, although the only carcinomas in

Correspondence to: Dr Kazuya Shinmura, First Department of Pathology, Hamamatsu University School of Medicine, 1-20-1 Handayama, Higashi Ward, Hamamatsu 431-3192, Japan
E-mail: kzshinmu@hama-med.ac.jp

Key words: EML4, ALK, non-small cell lung carcinoma, fusion transcript, immunohistochemistry

which ALK fusions have been found thus far are NSCLCs, ALK fusions may be present in other types of carcinomas. However, no studies using the iAEP method, except a study by Takeuchi *et al* (13), have been published. Therefore, in the present study, we immunohistochemically evaluated a total of 302 NSCLCs and 291 gastric carcinomas for ALK expression using the iAEP method and then investigated RNA-available, immunohistochemically ALK-positive tumors for expression of EML4-, KIF5B- and TFG-ALK fusions.

Materials and methods

Surgical specimens. Samples of surgical specimens from 302 NSCLC and 291 gastric carcinoma patients who underwent surgery for their cancer at Hamamatsu University School of Medicine, University Hospital or Mikatahara Seirei General Hospital were obtained. The mean age of the 302 NSCLC patients was 63.9 years [standard deviation (SD) 10.7], and they consisted of 168 men and 134 women. The NSCLC tumors were histologically classified as adenocarcinoma in 184 cases, squamous cell carcinoma in 98 cases, large-cell carcinoma in 9 cases and adenosquamous carcinoma in 11 cases. The mean age of the 291 gastric carcinoma patients was 65.4 years (SD 11.8), and they consisted of 206 men and 85 women. The gastric tumors were histologically classified as intestinal-type adenocarcinoma in 151 cases, diffuse-type adenocarcinoma in 138 cases and adenosquamous carcinoma in 2 cases. This study was approved by the Institutional Review Board (IRB) of Hamamatsu University School of Medicine and the IRB of Mikatahara Seirei General Hospital.

Immunohistochemical staining. Immunostaining for ALK using the iAEP method was performed as described previously (13) with slight modifications. In brief, paraffin-embedded tissue sections were deparaffinized, rehydrated and boiled at 96°C for 40 min in Target Retrieval Solution (pH 9.0) (Dako, Kyoto, Japan) for antigen retrieval. Endogenous peroxidase activity was blocked by incubation for 5 min in a 3% hydrogen peroxide solution. Next, the sections were incubated with a Protein Block, Serum-free (Dako) for 10 min at room temperature (RT) and then with a mouse anti-ALK monoclonal antibody (clone 5A4; Abcam, Cambridge, UK) at a dilution of 1:50 for 30 min at RT. To increase the sensitivity of detection, the sections were incubated with polyclonal rabbit anti-mouse immunoglobulin at a dilution of 1:500 for 15 min at RT. After washing, the sections were incubated for 30 min at RT with an amino acid polymer conjugated with goat anti-rabbit IgG and horseradish peroxidase (Histofine Simple Stain MAX-PO Kit; Nichirei, Tokyo, Japan). The antigen-antibody complex was visualized with 3,3'-diaminobenzidine tetrahydrochloride, and the sections were counterstained with hematoxylin. The staining was performed with a Dako autostainer (Dako) (20).

Reverse transcription (RT)-polymerase chain reaction (PCR). Total RNA was extracted from lung tissue samples with an RNeasy Kit (Qiagen, Valencia, CA, USA) and converted to first-strand cDNA with a SuperScript First-Strand Synthesis System for RT-PCR (Invitrogen, Carlsbad, CA, USA) by following the supplier's protocol. PCR was performed in 20-μl reaction mixtures containing HotStarTaq DNA polymerase (Qiagen) under the following conditions: 30 sec at 94°C, 30 sec at 61°C and 90 sec at 72°C for 45 cycles. A total of five different PCR primer pairs for EML4-ALK, three PCR primer pairs for KIF5B-ALK and one PCR primer pair for TFG-ALK were used for the RT-PCR. The forward PCR primers were: 5'-GCC TCA GTG AAA AAA TCA GTC TCA AG-3' for the sequence on exon 2 of EML4, 5'-ACA AAT TCG AGC ATC ACC TTC TCC-3' for the sequence on exon 4 of EML4, 5'-GTG CAG TGT TTA GCA TTC TTG GGG-3' for the sequence on exon 13 of EML4, 5'-CTG TGG GAT CAT GAT CTG AAT CCT G-3' for the sequence on exon 14 of EML4, 5'-CTT CCT GGC TGT AGG ATC TCA TGA C-3' for the sequence on exon 19 of EML4, 5'-CAC TAT TGT AAT TTG CTG CTC TCC ATC ATC-3' for the sequence on exon 10 of KIF5B, 5'-AAT CTG TCG ATG CCC TCA GTG AAG-3' for the sequence on exon 17 of KIF5B, 5'-TGA TCG CAA ACG CTA TCA GCA AG-3' for the sequence on exon 24 of KIF5B and 5'-TCG TTT ATT GGA TAG CTT GGA ACC AC-3' for the sequence on exon 4 of TFG. The reverse PCR primer used was the same, i.e., 5'-GAG GTC TTG CCA GCA AAG CAG TAG-3' for the sequence on exon 20 of ALK. The PCR products were fractionated by electrophoresis on an agarose gel and stained with ethidium bromide. The PCR-amplified products were purified with a PCR purification kit (Qiagen) and directly sequenced with a BigDye Terminator Cycle Sequencing Reaction Kit (Applied Biosystems, Tokyo, Japan) and the ABI 3100 Genetic Analyzer (Applied Biosystems) as described previously (7). The reference sequences for the *ALK*, *EML4*, *KIF5B* and *TFG* genes are accession numbers NM_004304, NM_019063, NM_004521 and NM_006070, respectively.

Statistical analysis. Statistical comparisons were performed by the two-tailed Student's t-test with Excel software (Microsoft Corp., Redmond, WA, USA).

Results

Immunohistochemical detection of ALK-positive NSCLCs. Samples of 302 NSCLCs and 291 gastric carcinomas were immunohistochemically stained for ALK with 5A4 anti-ALK monoclonal antibody using the iAEP method, and 12 (4.0%) of the NSCLCs and none (0%) of the gastric carcinomas were positive for ALK expression (Table I). ALK staining was observed in the cytoplasm of the cancer cells in all 12 NSCLCs, but not in any of the non-cancerous cells (Fig. 1). The mean age of the NSCLC patients whose tumors were positive for ALK was 57.3 years (SD 15.7) and significantly lower than the mean age of the NSCLC patients whose tumors were negative for ALK (64.2 years of age, SD 10.4) ($p=0.027$). The NSCLC patients whose tumors were positive for ALK consisted of 6 men and 6 women, and the ALK-positive NSCLC tumors were classified histologically as adenocarcinoma in 10 cases, adenosquamous carcinoma in 1 case and squamous cell carcinoma in 1 case (Table I).

Detection of various EML4-ALK fusion transcripts in NSCLCs. Next, 10 RNA-available, ALK-positive NSCLCs were investigated for expression of EML4-, KIF5B- and TFG-ALK fusion transcripts by RT-PCR and subsequent sequencing

Table I. Clinicopathological information and EML4-ALK fusions detected in immunohistochemically ALK-positive NSCLCs.

No.	Age	Gender	Histopathological diagnosis	EML4-ALK transcript
1	48	Female	Adenocarcinoma	Variant 1
2	49	Male	Adenocarcinoma	Variant 1
3	66	Male	Adenocarcinoma	Variant 1
4	46	Female	Adenocarcinoma	Variant 2
5	57	Male	Adenocarcinoma	Variant 2
6	79	Male	Adenocarcinoma	Variant 2
7	33	Female	Adenosquamous carcinoma	Variants 3a and 3b
8	63	Female	Adenocarcinoma	Variants 3a and 3b
9	83	Male	Adenocarcinoma	Variants 3a and 3b
10	58	Male	Adenocarcinoma	A novel variant[a]
11	36	Female	Adenocarcinoma	Not examined[b]
12	69	Female	Squamous cell carcinoma	Not examined[b]

[a]Exon 14 of EML4 is connected to a 2-bp fragment that in turn is ligated to the nucleotide at position 53 of exon 20 of ALK. [b]Due to the absence of an RNA sample, RT-PCR analysis for ALK fusions was not performed.

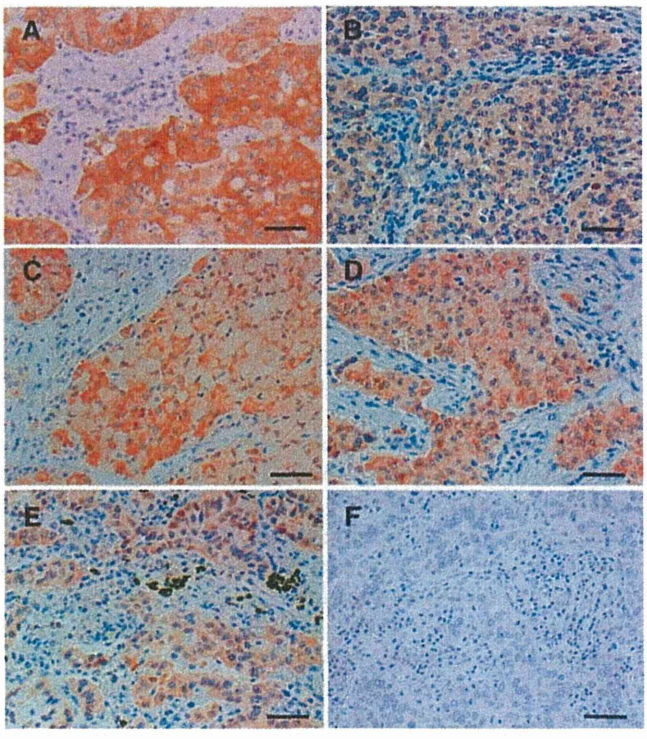

Figure 1. Representative results of immunohistochemical staining for ALK in non-small cell lung carcinomas. ALK protein expression was detected with 5A4 anti-ALK monoclonal antibody by the intercalated antibody-enhanced polymer method. A, B, C, D and E are the adenocarcinomas in cases No. 2, 5, 6, 8 and 10, respectively. F is the adenocarcinoma which showed no ALK expression. Bar, 50 μm.

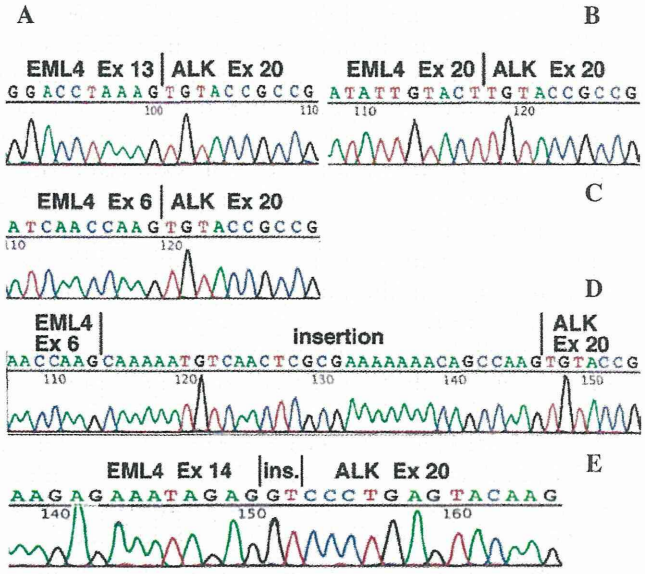

Figure 2. Detection of EML4-ALK fusion transcripts in non-small cell lung carcinomas. (A) EML4-ALK variant 1 transcript detected in case No. 1. (B) EML4-ALK variant 2 transcript detected in case No. 4. (C and D) EML4-ALK variants 3a (C) and 3b (D) transcripts detected in case No. 7. (E) Novel EML4-ALK transcript variant detected in case No. 10.

analyses. As a negative control, we also performed an RT-PCR analysis of 30 randomly selected, immunohistochemically ALK-negative NSCLCs. No expression of KIF5B-ALK or TFG-ALK fusion transcripts was detected in any of the carcinomas, but EML4-ALK fusion transcripts were detected in all 10 RNA-available, ALK-positive NSCLCs (Table I). As expected, no RT-PCR products were detected in any of the 30 immunohistochemically ALK-negative NSCLCs. Regarding the type of the EML4-ALK transcript, in 3 cases (No. 1-3) the fusion was variant 1, a fusion between exon 13 of EML4 and exon 20 of ALK (Fig. 2A), and in 3 cases (No. 4-6) it was variant 2, a fusion between exon 20 of EML4 and exon 20 of ALK (Fig. 2B). In 3 other cases (No. 7-9) the RT-PCR analysis yielded two bands, and they corresponded to variant 3a, a fusion between exon 6 of EML4 and exon 20 of ALK (Fig. 2C), and variant 3b, a fusion containing an additional 33-bp sequence derived from intron 6 of EML4 between exon 6 of EML4 and exon 20 of ALK (Fig. 2D). Notably, in case No. 10,

sequencing of the RT-PCR product revealed that exon 14 of EML4 was connected to an unidentified 2-bp fragment that was in turn ligated to the nucleotide at position 53 of exon 20 of ALK (Fig. 2E). The EML4-ALK sequence detected in case No. 10 allows an in-frame connection between the two genes and is a novel variant. The mean age of the 10 NSCLC patients whose tumors contained EML4-ALK transcripts was 58.2 years (SD 15.3), and they consisted of 6 men and 4 women. The NSCLC tumors containing EML4-ALK transcripts were histologically classified as adenocarcinoma in 9 cases and adenosquamous carcinoma in 1 case. These findings suggest that the iAEP method is useful for screening paraffin-embedded tissue sections for NSCLCs containing ALK fusion transcripts.

Discussion

Immunohistochemical screening for ALK expression using the iAEP method in the present study revealed an immunohistochemical ALK signal in 12 (4.0%) of 302 NSCLCs but not in any of the 291 gastric carcinomas. The ALK signal was detected in the cytoplasm of the cancer cells in all of the ALK-positive NSCLCs. RT-PCR and subsequent sequencing analyses of RNA from the 10 RNA-available, ALK-positive NSCLCs revealed the EML4-ALK variant 1 in 3 cases, variant 2 in 3 cases, both variants 3a and 3b in 3 cases, and a novel variant consisting of a fusion between exon 14 of EML4 and a nucleotide within exon 20 of ALK in 1 case. These results suggest that the immunohistochemistry-based system is useful for screening NSCLCs for ALK fusions, and identification of a novel EML4-ALK variant would be helpful in diagnosing NSCLCs containing ALK fusions in the future.

The proportion of immunohistochemically ALK-positive NSCLCs in this study (4.0%) is almost the same as the proportions of NSCLCs containing ALK fusion transcripts reported in previous studies (4,6-18), and in the present study EML4-ALK variants were detected in all RNA-available, immunohistochemically ALK-positive NSCLCs. These results suggest that our immunohistochemical analysis was performed properly and that the iAEP method with 5A4 anti-ALK antibody is a useful diagnostic tool for screening for NSCLCs containing ALK fusion proteins.

The histopathological diagnosis of 10 of the 12 immunohistochemically ALK-positive NSCLCs and 9 of the 10 EML4-ALK-positive NSCLCs in this study was adenocarcinoma. The predominance of adenocarcinomas among EML4-ALK-positive NSCLCs is consistent with the results of previous studies (6,12). This finding is also consistent with the recent finding of the growth of hundreds of adenocarcinoma nodules in transgenic mice in which EML4-ALK mRNA was transcribed specifically in lung epithelial cells (21). In the present study the mean age of the patients with immunohistochemically ALK-positive NSCLCs was significantly lower than that of the patients with ALK-negative NSCLCs. Although the mechanism responsible for the age difference is unknown, early onset may be a characteristic of ALK fusion-positive NSCLCs.

A novel EML4-ALK variant was found in this study. In this novel variant, exon 14 of EML4 was connected to a 2-bp fragment that was in turn ligated to the nucleotide at position 53 of exon 20 of ALK. Notably, the connection in each of two EML4-ALK variants, 4 and 7, is known to be between exon 14 of EML4 and a nucleotide within exon 20 of ALK (11,13). In variant 4, exon 14 of EML4 is connected to an unidentified 11-bp cDNA fragment that in turn is ligated to the nucleotide at position 50 of exon 20 of ALK (11), while in variant 7, exon 14 of EML4 is connected to the nucleotide at position 13 of exon 20 of ALK (13). Thus, the variant identified in this study is the third variant with a connection between exon 14 of EML4 and a nucleotide within exon 20 of ALK. Connections located within, rather that at the 5' terminus of, exon 20 of ALK have also been reported in MSN-ALK and MYH9-ALK, both of which have been detected in anaplastic large-cell lymphoma (22,23). Since a systemic understanding of the ALK fusions is important to correctly diagnose NSCLCs containing ALK fusions, our identification of a novel EML4-ALK variant should contribute to establishing a practical and accurate diagnostic system in the future.

Since the intracellular region of ALK was used as the antigen to produce the 5A4 anti-ALK antibody used in this study, both EML4-ALK and wild-type ALK should have been detected by the antibody. Takeuchi *et al* attempted to determine whether both transcripts are expressed by quantitatively analyzing the amount of mRNA specific for wild-type ALK and ALK fusion transcript separately, and found that none of the EML4-ALK-positive tumors yielded a substantial amount of wild-type ALK mRNA (13). Thus, immunohistochemical staining with the 5A4 antibody using the iAEP method appears to detect ALK fusion proteins and not wild-type ALK in NSCLCs. Our results for detection of EML4-ALK variants in all of the RNA-available, immunohistochemically ALK-positive NSCLCs support this view.

Our immunohistochemical analysis did not detect ALK protein expression in any of the gastric carcinomas. This was the first search for ALK fusion proteins in gastric carcinomas, and the results clearly demonstrated the absence of ALK fusion in gastric carcinomas. Since previous RNA analyses showed no EML4-ALK transcripts in 96 gastric carcinomas (8) and 33 gastric carcinomas (11), our results are consistent. The only human carcinomas in which ALK fusions have ever been found are NSCLCs. However, since it is unknown whether ALK fusions are involved in the genesis and development of other types of carcinoma, it may be worth investigating various types of carcinomas for expression of ALK fusion proteins in the future.

Acknowledgements

We are grateful to Dr K. Takeuchi (Cancer Inst, JFCR) for his technical advice regarding the iAEP method. This study was supported, in part, by a Grant-in-Aid from the Ministry of Health, Labour and Welfare for the Comprehensive 10-Year Strategy for Cancer Control (19-19), by a Grant-in-Aid from the Japan Society for the Promotion of Science for Scientific Research (no. 19790286), by a Grant-in-Aid from the Ministry of Education, Culture, Sports, Science and Technology of Japan on Priority Area (no. 18014009), by the 21st century COE program 'Medical Photonics' and by the Smoking Research Foundation.

References

1. Look AT: Oncogenic transcription factors in the human acute leukemias. Science 278: 1059-1064, 1997.
2. Lucansky V, Sobotkova E, Tachezy R, Duskova M and Vonka V: DNA vaccination against bcr-abl-positive cells in mice. Int J Oncol 35: 941-951, 2009.
3. Tomlins SA, Rhodes DR, Perner S, Dhanasekaran SM, Mehra R, Sun XW, Varambally S, Cao X, Tchinda J, Kuefer R, Lee C, Montie JE, Shah RB, Pienta KJ, Rubin MA and Chinnaiyan AM: Recurrent fusion of TMPRSS2 and ETS transcription factor genes in prostate cancer. Science 310: 644-648, 2005.
4. Soda M, Choi YL, Enomoto M, Takada S, Yamashita Y, Ishikawa S, Fujiwara S, Watanabe H, Kurashina K, Hatanaka H, Bando M, Ohno S, Ishikawa Y, Aburatani H, Niki T, Sohara Y, Sugiyama Y and Mano H: Identification of the transforming EML4-ALK fusion gene in non-small cell lung cancer. Nature 448: 561-566, 2007.
5. Verdorfer I, Fehr A, Bullerdiek J, Scholz N, Brunner A, Krugmann J, Hager M, Haufe H, Mikuz G and Scholtz A: Chromosomal imbalances, 11q21 rearrangement and MECT1-MAML2 fusion transcript in mucoepidermoid carcinomas of the salivary gland. Oncol Rep 22: 305-311, 2009.
6. Mano H: Non-solid oncogenes in solid tumors: EML4-ALK fusion genes in lung cancer. Cancer Sci 99: 2349-2355, 2008.
7. Shinmura K, Kageyama S, Tao H, Bunai T, Suzuki M, Kamo T, Takamochi K, Suzuki K, Tanahashi M, Niwa H, Ogawa H and Sugimura H: EML4-ALK fusion transcripts, but no NPM-, TPM3-, CLTC-, ATIC-, or TFG-ALK fusion transcripts, in non-small cell lung carcinomas. Lung Cancer 61: 163-169, 2008.
8. Fukuyoshi Y, Inoue H, Kita Y, Utsunomiya T, Ishida T and Mori M: EML4-ALK fusion transcript is not found in gastrointestinal and breast cancers. Br J Cancer 98: 1536-1539, 2008.
9. Choi YL, Takeuchi K, Soda M, Inamura K, Togashi Y, Hatano S, Enomoto M, Hamada T, Haruta H, Watanabe H, Kurashina K, Hatanaka H, Ueno T, Takada S, Yamashita Y, Sugiyama Y, Ishikawa Y and Mano H: Identification of novel isoforms of the EML4-ALK transforming gene in non-small cell lung cancer. Cancer Res 68: 4971-4976, 2008.
10. Perner S, Wagner PL, Demichelis F, Mehra R, Lafargue CJ, Moss BJ, Arbogast S, Soltermann A, Weder W, Giordano TJ, Beer DG, Rickman DS, Chinnaiyan AM, Moch H and Rubin MA: EML4-ALK fusion lung cancer: a rare acquired event. Neoplasia 10: 298-302, 2008.
11. Takeuchi K, Choi YL, Soda M, Inamura K, Togashi Y, Hatano S, Enomoto M, Takada S, Yamashita Y, Satoh Y, Okumura S, Nakagawa K, Ishikawa Y and Mano H: Multiplex reverse transcription-PCR screening for EML4-ALK fusion transcripts. Clin Cancer Res 14: 6618-6624, 2008.
12. Inamura K, Takeuchi K, Togashi Y, Hatano S, Ninomiya H, Motoi N, Mun MY, Sakao Y, Okumura S, Nakagawa K, Soda M, Choi YL, Mano H and Ishikawa Y: EML4-ALK lung cancers are characterized by rare other mutations, a TTF-1 cell lineage, an acinar histology and young onset. Mod Pathol 22: 508-515, 2009.
13. Takeuchi K, Choi YL, Togashi Y, Soda M, Hatano S, Inamura K, Takada S, Ueno T, Yamashita Y, Satoh Y, Okumura S, Nakagawa K, Ishikawa Y and Mano H: KIF5B-ALK, a novel fusion oncokinase identified by an immunohistochemistry-based diagnostic system for ALK-positive lung cancer. Clin Cancer Res 15: 3143-3149, 2009.
14. Martelli MP, Sozzi G, Hernandez L, Pettirossi V, Navarro A, Conte D, Gasparini P, Perrone F, Modena P, Pastorino U, Carbone A, Fabbri A, Sidoni A, Nakamura S, Gambacorta M, Fernández PL, Ramirez J, Chan JK, Grigioni WF, Campo E, Pileri SA and Falini B: EML4-ALK rearrangement in non-small cell lung cancer and non-tumor lung tissues. Am J Pathol 174: 661-670, 2009.
15. Rikova K, Guo A, Zeng Q, Possemato A, Yu J, Haack H, Nardone J, Lee K, Reeves C, Li Y, Hu Y, Tan Z, Stokes M, Sullivan L, Mitchell J, Wetzel R, Macneill J, Ren JM, Yuan J, Bakalarski CE, Villen J, Kornhauser JM, Smith B, Li D, Zhou X, Gygi SP, Gu TL, Polakiewicz RD, Rush J and Comb MJ: Global survey of phosphotyrosine signaling identifies oncogenic kinases in lung cancer. Cell 131: 1190-1203, 2007.
16. Koivunen JP, Mermel C, Zejnullahu K, Murphy C, Lifshits E, Holmes AJ, Choi HG, Kim J, Chiang D, Thomas R, Lee J, Richards WG, Sugarbaker DJ, Ducko C, Lindeman N, Marcoux JP, Engelman JA, Gray NS, Lee C, Meyerson M and Jänne PA: EML4-ALK fusion gene and efficacy of an ALK kinase inhibitor in lung cancer. Clin Cancer Res 14: 4275-4283, 2008.
17. Horn L and Pao W: EML4-ALK: honing in on a new target in non-small cell lung cancer. J Clin Oncol 27: 4232-4235, 2009.
18. Shaw AT, Yeap BY, Mino-Kenudson M, Digumarthy SR, Costa DB, Heist RS, Solomon B, Stubbs H, Admane S, McDermott U, Settleman J, Kobayashi S, Mark EJ, Rodig SJ, Chirieac LR, Kwak EL, Lynch TJ and Iafrate AJ: Clinical features and outcome of patients with non-small cell lung cancer who harbor EML4-ALK. J Clin Oncol 27: 4247-4253, 2009.
19. McDermott U, Iafrate AJ, Gray NS, Shioda T, Classon M, Maheswaran S, Zhou W, Choi HG, Smith SL, Dowell L, Ulkus LE, Kuhlmann G, Greninger P, Christensen JG, Haber DA and Settleman J: Genomic alterations of anaplastic lymphoma kinase may sensitize tumors to anaplastic lymphoma kinase inhibitors. Cancer Res 68: 3389-3395, 2008.
20. Shinmura K, Iwaizumi M, Igarashi H, Nagura K, Yamada H, Suzuki M, Fukasawa K and Sugimura H: Induction of centrosome amplification and chromosome instability in p53-deficient lung cancer cells exposed to benzo[a]pyrene diol epoxide (B[a]PDE). J Pathol 216: 365-374, 2008.
21. Soda M, Takada S, Takeuchi K, Choi YL, Enomoto M, Ueno T, Haruta H, Hamada T, Yamashita Y, Ishikawa Y, Sugiyama Y and Mano H: A mouse model for EML4-ALK-positive lung cancer. Proc Natl Acad Sci USA 105: 19893-19897, 2008.
22. Tort F, Pinyol M, Pulford K, Roncador G, Hernandez L, Nayach I, Kluin-Nelemans HC, Kluin P, Touriol C, Delsol G, Mason D and Campo E: Molecular characterization of a new ALK translocation involving moesin (MSN-ALK) in anaplastic large cell lymphoma. Lab Invest 81: 419-426, 2001.
23. Lamant L, Gascoyne RD, Duplantier MM, Armstrong F, Raghab A, Chhanabhai M, Rajcan-Separovic E, Raghab J, Delsol G and Espinos E: Non-muscle myosin heavy chain (MYH9): a new partner fused to ALK in anaplastic large cell lymphoma. Genes Chromosomes Cancer 37: 427-432, 2003.

Journal of Human Genetics (2010) 0, 1–6

www.nature.com/jhg

ORIGINAL ARTICLE

Association between neuropeptide Y receptor 2 polymorphism and the smoking behavior of elderly Japanese

Naomi Sato[1,2], Shinji Kageyama[1], Renyin Chen[1,4], Masaya Suzuki[1], Hiroki Mori[1], Fumihiko Tanioka[3], Hidetaka Yamada[1], Takaharu Kamo[1], Hong Tao[1], Kazuya Shinmura[1], Akiko Nozawa[2] and Haruhiko Sugimura[1]

Molecular heterogeneity of neuropeptide Y (NPY) and its three receptors (1, 2 and 5) has recently been discovered. *NPY2R* polymorphisms have been shown to be related to cocaine and alcohol dependence in European Americans. To test our hypothesis that these polymorphisms influence the smoking behavior of Japanese population, we investigated the prevalence of the rs4425326 and rs6857715 polymorphisms, which have been suggested to be related to alcohol dependence in European Americans, in 2517 Japanese elderly subjects for whom information on smoking behaviors was available. The prevalence of current smokers was greater among Japanese men having the rs4425326 C allele than ex-smokers. Among the ever-smokers, the Fagerström Test for Nicotine Dependence scores were higher in men having the rs4425326 homozygous T allelotype, and the numbers of cigarettes smoked per day were also significantly higher in the male smokers having the TT genotype. No correlations between the Tobacco Dependence Screener scores and any genotypes were detected. These results suggest that rs4425326 polymorphisms may be related to smoking behavior in the Japanese elderly population. This study for the first time suggests NPY2R genotype as a possible genetic factor in nicotine dependence.
Journal of Human Genetics (2010) **0**, 000–000. doi:10.1038/jhg.2010.108

Keywords: addiction; Fagerström Test for Nicotine Dependence (FTND); neuropeptide Y (NPY); *NPY2R*; single nucleotide polymorphism; smoking behavior; Tobacco Dependence Screener (TDS); nicotine dependence

INTRODUCTION

Neuropeptide Y (NPY) is a neuromodulator in the leptin–melanocortin axis. There are three types of receptors of NPY receptors (NPYRs) in humans: NPY receptor type 1 (NPY1R), NPY receptor type 2 (NPY2R) and NPY receptor type 5 (NPY5R). They are all G-protein-coupled receptors having a 7-transmembrane domain,[1] and the genes that encode them are located on chromosome 4.

The physiological and pathological functions of NPY and NPYRs have been widely investigated in relation to the pathogenesis of obesity (food-seeking behavior),[2] hypertension[3] and other neurovascular disorders.[4] Some psychological conditions have recently been claimed to be related to the NPY–NPYR system,[5] and the claim has generated controversy.[6] Abuse of several substances, including methamphetamine, phencyclidine, cocaine, marijuana and alcohol, is thought to be associated with the NPY–NPYR axis.[7] Polymorphisms in the *NPY* gene locus (chromosome 7) and *NPY* receptor loci are known, and they are currently being investigated for possible associations with individual differences in addictive behaviors. The *NPY* locus polymorphism has been extensively studied in regard to various aspects of many physiological and psychological disorders. For example, the Leu7Pro (rs16139) single nucleotide polymorphism (SNP) has been reported to be associated with alcohol consumption and the alcohol withdrawal syndrome in a European-American population.[8–10] However, it has a different prevalence in several other populations besides a European-American population,[11] and the association was not reproducible in Swedes and Finns.[12] Other polymorphisms in the *NPY* gene have been also reported to be related to alcohol dependence/preference.[13–15]

The roles of variants of the NPYRs, however, have not been thoroughly investigated. Wetherill *et al.*[16] carried out an extensive investigation of polymorphisms of *NPY* and *NPY* receptors: 7 SNPs in *NPY*, 15 SNPs in *NPY2R* including the 5′ end, and 17 SNPs in *NPY1R* and *NPY5R* in alcohol-dependent population; in populations with various degrees of the alcohol withdrawal syndrome and in populations with cocaine dependence. They found that several polymorphisms, including rs4425326 and rs6857715 located in the upstream of

[1]Department of Pathology, Hamamatsu University School of Medicine, Hamamatsu, Shizuoka, Japan; [2]Department of Clinical Nursing, Hamamatsu University School of Medicine, Hamamatsu, Shizuoka, Japan and [3]Division of Pathology and Laboratory Medicine, Iwata City Hospital, Iwata, Japan
[4]Current address: Department of Pathology, Zhengzhou University, Zhengzhou, PR China.
Correspondence: Dr H Sugimura, Department of Pathology, Hamamatsu University School of Medicine, 1-20-1, Handayama, Higashi-ward, Hamamatsu, Shizuoka 431-3192, Japan.
E-mail: hsugimur@hama-med.ac.jp
Received 12 May 2010; revised 1 August 2010; accepted 5 August 2010